NASA CR-72056
LAC ER-8673

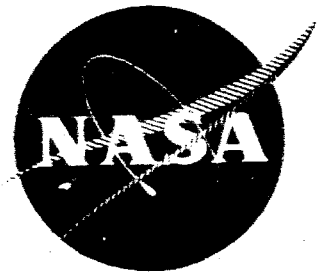

EFFECT OF NUCLEAR RADIATION ON MATERIALS AT CRYOGENIC TEMPERATURES

by

LOCKHEED NUCLEAR PRODUCTS

C. A. Schwanbeck, Project Manager

prepared for

NATIONAL AERONAUTICS AND SPACE ADMINISTRATION

Contract NAS3–7985

LOCKHEED NUCLEAR PRODUCTS

NOTICE

This report was prepared as an account of Government sponsored work. Neither the United States, nor the National Aeronautics and Space Administration (NASA), nor any person acting on behalf of NASA:

A.) Makes any warranty or representation, expressed or implied, with respect to the accuracy, completeness, or usefulness of the information contained in this report, or that the use of any information, appartus, method, or process disclosed in this report may not infringe privately owned rights; or

B.) Assumes any liabilities with respect to the use of, or for damages resulting from the use of any information, apparatus, method or process disclosed in this report.

As used above, "person acting on behalf of NASA" includes any employee or contractor of NASA, or employee of such contractor, to the extent that such employee or contractor of NASA, or employee of such contractor prepares, disseminates, or provides access to, any information pursuant to his employment or contract with NASA, or his employment with such contractor.

Requests for copies of this report should be referred to

National Aeronautics and Space Administration
Office of Scientific and Technical Information
Attention: AFSS-A
Washington, D.C. 20546

NASA CR-72056
LAC ER-8673

QUARTERLY REPORT NO. 4

April 21, 1966 Through July 21, 1966

EFFECT OF NUCLEAR RADIATION ON MATERIALS AT CRYOGENIC TEMPERATURES

by

LOCKHEED NUCLEAR PRODUCTS

C. A. Schwanbeck, Project Manager

prepared for

NATIONAL AERONAUTICS AND SPACE ADMINISTRATION

August 1966

Contract NAS 3-7985

Technical Management
NASA Lewis Research Center
Cleveland, Ohio
Nuclear Systems Division
Charles L. Younger

LOCKHEED NUCLEAR PRODUCTS
LOCKHEED-GEORGIA COMPANY

A DIVISION OF LOCKHEED AIRCRAFT CORPORATION

If this document is supplied under the requirements of a United States Government contract, the following legend shall apply unless the letter U appears in the coding box:

This data is furnished under a United States Government contract and only those portions hereof which are marked (for example, by circling, underscoring or otherwise) and indicated as being subject to this legend shall not be released outside the Government (except to foreign governments, subject to these same limitations), nor be disclosed, used, or duplicated, for procurement or manufacturing purposes, except as otherwise authorized by contract, without the permission of Lockheed-Georgia Company, A Division of Lockheed Aircraft Corporation, Marietta, Georgia. This legend shall be marked on any reproduction hereon in whole or in part.

The "otherwise marking" and "indicated portions" as used above shall mean this statement and includes all details or manufacture contained herein respectively.

Code: U	Contract: NAS 3-7985

FOREWORD

This quarterly report is submitted to the National Aeronautics and Space Administration, Lewis Research Center, by the Lockheed-Georgia Company in accordance with the requirements of NASA Contract NAS 3-7985.

TABLE OF CONTENTS

TABLE OF CONTENTS (Cont'd)

TABLE OF CONTENTS (Cont'd)

1 SUMMARY

This is the fourth quarterly report summarizing the work to date on Contract NAS 3-7985 entitled, "The Effect of Nuclear Radiation on Material at Cryogenic Temperatures." The studies under this contract include the effects of (1) 10^{18} n/cm2 (E > 0.5 MeV) at 30°R on tensile properties of titanium base alloys; (2) irradiation temperature (30°R to 540°R) on tensile properties of Aluminum 1099-H14 following irradiations up to 3×10^{17} n/cm^2 (E > 0.5 MeV); (3) annealing following irradiation at 30°R to 10^{17} n/cm^2 (E > 0.5 MeV) on tensile properties of Aluminum 1099; and (4) irradiation at 30°R on axial, low-cycle fatigue properties of titanium base alloys.

The tensile testing phase of the contract is being performed with government owned test equipment which was available at the beginning of the contract. All out-of-pile tensile testing and in-pile testing of Aluminum 1099, Ti-55A, Ti-5Al-2.5 Sn (ELI) and Ti-6Al-4V (Annealed) has been completed.

The recovery for the previously reported cryogenic depression of the F_{ty}/F_{tu} ratio in Aluminum 1099-H14 (unirradiated) was observed to be an essentially linear function of irradiation level. After 3×10^{17} n/cm^2 (E > 0.5 MeV), this parameter at 30°R is over 70% of its initial room temperature value, indicating a similarity between irradiation effect and work hardening. It was observed that there was no significant difference between the mechanical properties of Aluminum 1099 after irradiation to 10^{17} n/cm^2 (E > 0.5 MeV) at 30°R followed by annealing and testing at several higher temperatures, and the same properties from specimens, both irradicted to 10^{17} n/cm^2 (E > 0.5 MeV) and tested at the higher temperatures. However, significant variation was observed between the residual irradiation effects after annealing when tested at the annealing temperature and when re-cooled to the irradiation temperature prior to test.

Increases in strength functions, accompanied by moderate reductions in ductility were observed in the three titanium alloys for which testing was complete. There was no evidence of saturation at 10^{18} n/cm2 (E > 0.5 MeV).

The low-cycle fatigue testing phase has required extensive modification of the hydraulic load control system and some changes to the test loops. Required new components have been fabricated or purchased and have been installed. The electronics portion of the system has been operated in a preliminary manner under cyclic operation and methods of calibrating are being developed.

2 INTRODUCTION

The combination of a fast neutron and cryogenic environment encountered in the structural members of a liquid hydrogen nuclear rocket imposes service conditions dissimilar to those encountered in other engineering applications. Both fast neutron bombardment and extremely low temperatures affect the mechanical properties of engineering materials; therefore the magnitude of the combined effect must be determined to provide basic design information before materials for a reliable nuclear rocket system can be selected. Since the neutron irradiation effects will spontaneously anneal even at low temperatures, tests to provide the desired information concerning the combined effect must be conducted with the specimens held at the temperature of interest during the entire irradiation and testing period.

A screening program (ref. 1) was undertaken to assess the effect of fast neutron irradiation on selected engineering alloys at temperatures near the boiling point of liquid hydrogen (-423°F). Tensile tests on parallel sample sets of unnotched specimens for each alloy at room temperature unirradiated, at 30°R (-430°F) unirradiated and at 30°R irradiated to 1×10^{17} n/cm^2 ($E > 0.5$ MeV), were performed at the NASA Plum Brook Reactor Facility using a helium refrigerator and testing equipment specially designed for in-pile testing under controlled temperature conditions.

Test results from the screening program indicated that titanium alloys possessed the highest strength-to-weight ratio following exposure to the combined nuclear-cryogenic environment as well as being among the least susceptible to deterioration of mechanical properties of the alloys tested. On the other hand, Aluminum 1099 (99.99% Aluminum) was found to be very sensitive to both irradiation and temperature of irradiation.

Based on the information obtained from the screening program, an in-pile test program (see section 5) has been initiated to study in greater detail the effects of a combined nuclear-cryogenic environment on the mechanical properties of metals. The objective of this program is to provide engineering data at higher integrated fluxes and/or under different load conditions than heretofore attained at cryogenic temperatures as well as data for more fundamental studies. Its scope consists of two general phases, tensile testing and low-cycle fatigue testing. The tensile testing phase includes irradiations at 30°R to 10^{18} n/cm^2 ($E > 0.5$ MeV), irradiations to 10^{17} n/cm^2 ($E > 0.5$ MeV) at temperatures between 30°R and room temperature (540°R), and irradiations to 10^{17} n/cm^2 ($E > 0.5$ MeV) at 30°R followed by specimen warm-up prior to fracture. The low-cycle fatigue testing phase includes

both fatigue testing during irradiation at 30°R and fatigue testing following irradiation at 30°R to 10^{17} n/cm^2 (E > 0.5 MeV).

Standard test specimens cannot be used in this test program due to various restrictions on the test equipment imposed by the nuclear cryogenic environment. The tensile specimens being used represent a miniaturization of the standard ASTM E-8 specimen (ref. 3). The miniature fatigue specimens required in this program represent a departure from any commonly used design, but are similar in geometry to those used by other investigators (ref. 4).

Progress during the earlier reporting periods (refs. 5, 6 and 7) consisted of necessary preparations, neutron flux mapping, temperature correlations, some modifications of existing equipment, and some test results.

During this reporting period tensile testing of several of the materials was completed. Also test equipment modification for low-cycle fatigue testing was completed and out-of-pile fatigue testing was initiated.

3 TEST EQUIPMENT

The test equipment (figure 1) for in-pile and out-of-pile testing under controlled temperature and load conditions permits the test program to be performed wholly by remote operations. Most of this equipment had undergone major overhaul and modification (ref. 2) in preparation for the nominal 140 hours irradiation period to obtain 10^{18} n/cm^2 (E > 0.5 MeV) exposures. Maintenance and calibration schedules, established during this overhaul effort, have kept the equipment operating reliably. This equipment and its operation, described previously (refs. 1, 5, 6 and 7), is summarized in the following sections for purposes of discussing information pertinent to the design, modification, and performance characteristics.

3.1 TEST LOOPS

The test loops are stainless steel cylindrical envelopes, six inches OD by about nine feet long, containing all necessary equipment for irradiating a test specimen under controlled temperature conditions and fracturing the specimen, at temperature, in tension or compression without removal from the irradiation field. At the aft end of the test loops, fittings are provided to connect the refrigeration system, the load control system, and the instrumentation and data recording system. Other fittings are provided for test loop cooling using deionized water (which must be isolated from the helium refrigerant).

To perform the test program, five tension-compression test loops are currently being used as follows:

Test loop 201-001 (the prototype loop): design and maintenance studies

Test loop 201-002: in hot laboratory area where investigation of various methods of repairing the inner helium line are being evaluated (section 3.7.1)

Test loop 201-003: used during this reporting period for tensile testing

Test loop 201-004: used during this reporting period for tensile testing then modified for low-cycle fatigue testing

Test loop 201-005: modified during this reporting period and used for preliminary fatigue testing

3.1.1 Tensile Test Loops

During this reporting period, test loops 201-003 and 201-004 were used for a total of 30 cycles* in performing in-pile tensile tests. Test loop 201-003 (with head assembly 201-011) was used for 16 cycles of operation and test loop 201-004 (with head assembly 201-006) was used for 14 cycles of operation. Both of these loops performed satisfactorily; however, during one in-pile test, indication of leakage was observed in the evacuated space surrounding the refrigerant lines in loop 201-003. After completion of the reactor cycle the loop was positioned in the hot cave and a leak was located in the forward end of the loop. The leak was repaired remotely and subsequent testing indicated that the integrity of the vacuum space was re-established. There was no loss of irradiation time as a consequence of this required repair.

3.1.2 Fatigue Test Loops

Low-cycle axial tension-compression fatigue tests are to be performed using existing tension-compression test loops. The original specifications to which the test loops were constructed required that they be capable of exerting tensile or compressive loads, but not both in a cyclic manner. Therefore, the existing self-aligning features have been replaced by a more complex arrangement and considerable analysis and some modification has been required before reliable tensile-compressive fatigue data can be obtained.

The prototype tensile test loop (201-001) and tensile test loop 201-005 were used to experimentally determine the extent of modification required. After completion of the detail design and experimental evaluation of the fatigue loop concepts in these test loops, similar modifications were performed on loop 201-004.

---

* For cycle definition, see section 3.7.

Results of these efforts to date are summarized in the following paragraphs:

Test Specimen Holders: For fatigue testing, specimen holders of the design shown in figure 2 will be used. This design is based on the performance of prototype holders and jam nuts with matching conical faces for maximum specimen alignment and minimum slack due to variations in thread dimensions. The system was designed using the smallest number of parts possible to minimize lost motion. This design also meets heat transfer requirements in that heat flow through the specimen is minimized. Two sets of these holders have been used satisfactorily for many thousands of cycles at loads up to 3,000 pounds.

Test Loop Structural Member Assembly Deflection: The structural member is the assembly installed in the test loop which supports the specimen loading actuator and also acts as a column directing the loads, which occur during loop insertion into the reactor beam port, into the carriage trunnion. The load applied in the test specimen is transmitted through the head assembly back through this member to the actuator. The load resulting from testing is distributed peripherally and transmitted eccentrically into the member. Deflection studies (ref. 5 and ref. 6) show that modification of the structural member of test loops 201-004 and 201-005 is not required.

Lost Motion in Pull Rod Linkage: The lost motion in the pull rod linkage of test loops 201-004 and 201-005 is assumed to be not significantly greater than the 0.02 inch measured in the prototype loop at 3500 pounds load (ref. 5). This assumption is based on the fact that the linkages are mechanically identical and has been confirmed by loading responses on going from tension to compression, similar to those with the prototype loop.

Hydraulic Actuator Seals: The hydraulic actuator seals have been qualified for cyclic operation to 10,000 cycles. During a previous reporting period, (ref. 5), over 1400 cycles at high loads with new seals, were obtained with

test loop 201-001 without indication of failure. During this reporting period, test loop 201-005 accumulated a total of over 70,000 cycles of operation at various loads.

Test Loop Head Assembly Organic Seals: The test loop head assembly organic seals for fatigue testing will be the same as those used for tensile testing. These seals will be subjected to more severe dynamic load conditions and some difficulties are anticipated, particularly with irradiation. No difficulties have been experienced so far during the preliminary cyclic loading at 30°R and 540°R out-of-pile. To date there has been no cyclic loading in-pile.

Test Loop Head Assemblies: Two new head assemblies have been ordered for the modified test loops which are to be used for in-pile testing. The most highly stressed member of each of these assemblies is being machined from Inconel 718 in place of Stainless Steel 304. Although a hazards analysis (section 3.8.1.3) shows the Stainless Steel 304 to be satisfactory, at least at moderate loads, this modification was made to provide a more than adequate endurance limit for fatigue testing at high loads.

Helium Ducts: An additional modification to the test loops required for the fatigue testing and accomplished during this reporting period was the adaptation of the helium ducts to fit the new specimen holders.

During this reporting period, test loop 201-005 was placed in service for fatigue testing. In the performance of out-of-pile testing at 30°R, a leak was detected in the refrigerant line vacuum jacket at the forward end of the test loop. The leak was found to be in a weld in an accessible position and was repaired. In addition, test loop 201-005 has been fitted with thermocouple lead wires in preparation for temperature correlation measurements from a fatigue specimen similar to those from a tensile specimen described in section 4.3.2.

3.2 REFRIGERATION SYSTEM

The test specimen temperature is maintained at temperatures between 30° - 540° Rankine using a gaseous phase helium refrigerator system. This system (ref. 5) contains an electrically driven positive displacement compressor, counterflow heat exchanger and four reciprocating expansion engines. The system was specifically designed and fabricated for this application to provide a minimum of 1150 watts of refrigeration for maintaining any specified specimen temperature from 30°R to 540°R by varying engine speed, expansion engine pressure ratio, and the heat input from manually controlled electrical resistance heaters installed in the refrigerant distribution manifold.

Some difficulty has been encountered in operating the system to provide the limited refrigeration required to dissipate gamma heat at 540°R (refs. 6 and 7). The engines, operating at low speed, stalled when contaminants in the helium collected and froze in the cylinders. The problem has been circumvented for the limited number of tests at 540°R in this program by using purge helium and bypassing the expansion engines.

During this reporting period, the system was operated for approximately 1050 hours and performed satisfactorily in conducting all scheduled in-pile and out-of-pile testing.

3.3 LOAD CONTROL SYSTEM

The existing specimen loading system for tensile testing utilizes a positive displacement pump with demineralized water as the working fluid to provide the pressure required by the hydraulic actuator positioned in the test loop. Strain rate can be controlled through a variable speed drive connected to the pump.

The load transducer is located in the test loop and the extensometer is positioned directly on the specimen to measure only the strain which occurs between the gage marks. The pump and recording instrumentation are located in appropriate cabinets positioned on the grating above the quadrant at the 0'-0" level.

To perform the low-cyclic fatigue studies this system has been modified (refs. 5 and 6) to provide a closed loop servo system as shown in figure 3. The modified system includes an oil operated actuator mechanically coupled to a demineralized water operated actuator, which in turn provides the required flow and pressure to the actuator installed in the test loop.

Installation, check-out and calibration of the system was completed during this reporting period.

Hydraulic system check-out included flushing of the system and testing of the installed hydraulic lines, under a pressure of 1.5 times actual operating pressures, with NASA observors in attendance. The oil side lines were tested at 4500 psig and the water side lines were tested at 1800 psig. The oil system was operated for several hours, pumping oil through the flushing block, before changing the line filters and switching the servo valve into the system.

The electronics portion of the system was first checked out under cyclic operation using a simulated load in place of the dynamometer LVDT signal, and an accurate method of calibrating the servo controller with respect to the command signal and output to the recorders was determined. Several dynamometers have been calibrated, using a new digital type voltmeter, for use in preliminary testing.

3.4 TRANSFER SYSTEM

To permit insertion and withdrawal of the test loops into the reactor, during reactor operation, a transfer system was designed and installed in quadrant D of the Plum Brook Reactor Facility. In addition, provision to change test specimens was incorporated by the installation of a hot cave with an access port in line with the assigned reactor beam port HB-2, as shown in figure 1.

To position the test loop for insertion or withdrawal from either the beam port or hot cave, the supporting tables, which are submerged approximately twenty feet in quadrant water, are aligned remotely using hydraulic pressure provided from an axial piston pump using demineralized water as a working fluid. After positioning, the loop carriage is coupled to the access port and the loop is inserted or withdrawn by a worm-drive screw arrangement driven by a hydraulic motor.

During this reporting period, the transfer system was used for a total of thirty cycles* of test loop insertion and removal. The system performed satisfactorily during this operational period.

3.5 SPECIMEN CHANGE EQUIPMENT

Due to the high activity level of the test loops after several in-pile exposures, remote handling techniques are required for changing specimens. A hot cave provides adequate shielding for this operation. This cave is provided with manipulators, support fixtures and special tools to permit change-over of the specimen. In addition, minor repairs on the forward end of the test loop have been performed in this hot cave.

During this reporting period, the specimen change equipment was used for installation and removal of thirty test specimens. No specimen change equipment difficulties were encountered.

3.6 MISCELLANEOUS TEST EQUIPMENT

During this reporting period, the test loop transfer cask and associated equipment were used to move a test loop to the hot laboratory area in accordance with approved procedures. Loop 201-004 was transferred to permit modification for fatigue testing.

3.7 TEST EQUIPMENT MAINTENANCE AND CALIBRATION

Projected maintenance schedules for the test equipment and refrigerator system define the major sub-systems associated with the test equipment and the components contained therein that require periodic scheduled inspection, adjustment, repair and overhaul. The maintenance and calibration program previously developedby a reliability analysis provided a use cycle and a common criterion for maintaining records of the use and performance of scheduled maintenance on the test equipment. The cycle is as follows:

---

* For cycle definition, see section 3.7.

- Insertion into hot cave for specimen installation.
- Removal from hot cave after specimen installation.
- Insertion into reactor beam port for test irradiation.
- Withdrawal from beam port after completing test, and positioning the loop for insertion into the hot cave for specimen change-over.

Normal operation of the test equipment follows this cycle. However, most of the equipment will operate submerged in the quadrant water, and with the exception of the carriages and test loops, is accessible for maintenance only when the quadrant is drained. Some deviations from the projected schedules are anticipated.

The projected refrigerator maintenance schedule is related to the hours of operation which are recorded cumulatively on a time meter which operates when the expansion engines are operating. Operating time is maintained by recording start-up and shut-down time on the refrigerator operation logs. Maintenance logs are used to record normal and abnormal maintenance and repair.

During this reporting period, the projected maintenance schedules were adhered to, inasmuch as possible, to perform routine inspection and repair. A number of repairs and adjustments were performed, some being a continuation of effort previously reported (refs. 6 and 7) and some required due to equipment malfunction during performance of the test program.

3.7.1 Test Loop Repairs

As previously reported (refs. 5, 6 and 7), leakage in one of the refrigerant lines was noted in test loop 201-002. Further efforts during this reporting period enabled a more precise determination of the position and nature of the leak. It appears to be a circumferential crack in the weld of the aft joint between the bellows assembly used to compensate for the change in length between the inner and outer helium lines and the inner wall of the annular vacuum space insulating the refrigerant lines.

Attempts were made, using mock-up test fixtures with manufactured defects, to determine a method of line repair in situ. One repair method tried was an attempt to fill the defect with a metallic coating deposited by commercially available

electro-chemical methods. Both copper and nickel were tried as coatings. Initial difficulty was encountered in obtaining a chemically clean surface for plating the ID of a stainless steel tube using methods feasible for remote techniques. A combination of electro-cleaning with alternating polarity and organic solvent chemical cleaning provided a surface on the tubing ID adequate for electro-plating. However, during deposition even at the lowest amperage available, the metal formed nodular dendritic growths at the edge of the discontinuity, forming craters rather than sealing the defect.

The electro-chemical approach was abandoned after this failure and several additional attempts were made to seal manufactured defects using epoxy and silicone sealants. Adequate room temperature sealing of the defects was obtained in several instances using these materials. However, in all cases leaks developed on thermal shocking with liquid nitrogen.

During this reporting period, new attempts were made to determine the feasibility of using epoxy type materials to repair the leak. Several successful repairs have been made on tube test pieces. These were thermal shocked in LN_2 with good results. Further effort is being directed toward a method of remotely applying the epoxy to the inside surface of the line, once the leak is precisely located.

As discussed in sections 3.1.1 and 3.1.2 both loops 201-003 and 201-005 developed leaks at their forward ends and were repaired during this reporting period.

3.7.2 Refrigeration System Repairs

The transfer lines terminate in a thermally isolated enclosure containing refrigerant shut-off and by-pass valves normally used to isolate the test loop from the refrigerant stream and to permit circulation of the refrigerant in the transfer lines to maintain them at low temperature during specimen change-over. These valves, in all three transfer line assemblies, have frequently malfunctioned or leaked so severely that they could not be used for their intended application, thus requiring the utilization of manually operated valves in the manifold to isolate the test loops. In addition, leaks occurred in the flexible portion of the transfer lines (refs. 5 and 6) resulting in a heat leak into the lines far exceeding the permissible rate.

Repair of the leaking transfer lines and modification of the valve chest assembly was in progress at the beginning of the reporting period. This work is being performed by the manufacturer and includes incorporation of soft seats in the valves and provision for seat replacement without cutting or welding of the valve chest as formally required.

One set of transfer lines was repaired and modified prior to this reporting period. A second set was completed during this reporting period and the third set has been shipped for modification and repair.

The main line heater, located in the refrigeration system manifold, burned out at the end of the last reporting period and was replaced during a long reactor shut down. The new element was apparently faulty and burned out after only a few hours of operation. Although not needed for forthcoming tests, this element will be replaced at the earliest opportunity.

An unscheduled refrigerator shut-down occured during an out-of-pile test in this reporting period. The cause was a broken oil line between the hydraulic motor and heat exchanger and the line was replaced.

During this reporting period repair and maintenance of the refrigerator included the overhaul of the crosshead assembly in engine pod number 2 and the purging of the refrigerator heat exchanger with freon solvent to eliminate residual contaminants.

3.7.3 Corrosion of Test Equipment

As previously reported in reference 6, evidence of corrosion had been observed in test head assembly 201-010. A corrosion engineer was consulted and new head assemblies are being acquired which incorporate numerous recommended design features. These include reducing the welding of thin gage metal, and cleaning and passivation consistent with total test loop design together with other improvements to minimize the possibility of deionized water contacting potential corrosion areas. Other features were not incorporated due to design implications on the test loop; however, the new features will minimize corrosion susceptability and result in increased head assembly life.

As discussed in detail in reference 6, the welded stainless steel actuator bellows assemblies which separate helium from cooling water in the test loops have exhibited corrosion at the welded peripheral seams. To alleviate this problem,

the welded bellows in the test loops will be replaced by two sections of two-ply hydraulically formed bellows, welded end-to-end and welded to suitable adapters at the ends. The end-to-end welding is required because the section lengths are limited by the forming technique. The spring rate of the new bellows assembly is about 22 lb/in.

The first replacement was made in the prototype loop to determine the best installation procedures before replacement of the bellows in the other loops. Following the replacement of a bellows in the prototype loop, a new bellows was installed in the non-irradiated test loop 201-005, to permit further refinement of the techniques. The methods developed provided leak-free joints in these loops. However, it remains to be determined if they are adequate for fabrication of leak-free welds in the limited working exposures permitted on the irradiated test loops. Replacement of the bellows in the irradiated test loops will not be attempted until necessitated by a bellows failure.

3.7.4 Miscellaneous Repairs and Adjustments

Carriage number 4 was removed from the quadrant for inspection and repair. The hydraulic motor was returned to the manufacturer for overhaul. On return of the motor, the carriage was reassembled, with a repaired wiring harness, and tested.

Inspection of the traverse bearing system of the north loop transfer table was performed during this reporting period.

3.8 EXPERIMENT DESIGN MANUAL AND HAZARDS ANALYSIS

As previously reported (ref. 5), revisions to the Experiment Design Manual and Hazards Analysis were required, since:

- The present test program includes irradiation exposures at 140°R, 320°R and 540°R, as well as at 30°R. Prior experiment approval from the Plum Brook Reactor Facility was predicated on operation at 30°R, freezing-out gaseous impurities in the refrigerant prior to irradiation of the gas.

- The present test program includes cyclic loading from tension to compression, thus changing the stress pattern on the test loop head from that used as a basis of the stress analysis on which prior experiment approval was based.

The modification of the Experiment Design Manual and Hazards Analysis required by the increased irradiation temperature was completed and reported in the preceding reporting period (ref. 6). These changes consisted of an activation analysis of the possible impurities in the refrigerant and determination of the degree of hazard incurred in the event of the maximum credable incident. The calculations and conclusions were included in the Experiment Design Manual and Hazards Analysis and the Plum Brook Reactor Facility has granted approval for experiment operation at all temperatures up to 540°R.

3.8.1 Analysis of Hazards Due to Cyclic Loading

A refined hazards analysis, including various components in the test loop, operating in tension and compression in cyclic loading up to a maximum of 3500 pounds load, was completed during this reporting period. The analysis is to determine if the head bolts, seal arrangement and the end cap of the head assembly are subject to fatigue failure under the most severe operating conditions and if such a failure could constitute a hazard to the reactor or test facility operation.

3.8.1.1 Head Bolt Failure

The head assembly is attached to the test loop by ten preloaded head bolts. During in-pile operation the forces to be considered with respect to possible head bolt failure are those due to the net hydraulic load on the head assembly and the maximum compressive load on the specimens. The helium within the head assembly is under approximately 35 psig pressure and the cooling water external to the head assembly is under approximately 135 psig so that the net hydraulic load on the head assembly is approximately 1885 pounds applied concentrically in the aft direction. The maximum compressive load applied to the specimen is 3500 pounds, applied eccentrically (0.627 inch off center) in the forward direction.

The net force of 1615 pounds will add to the tensile prestress of the bolts and subtract from the compressive load on the head assembly cylindrical section in the approximate proportion of their relative stiffness, 1:6.5. Considering the eccentricity of the specimen loading in a simple moment calculation this results in a stress of 1794 psi added to the prestress of approximately 18,050 psi in the critical bolt. This total of approximately 20,000 psi is well below the endurance limit so that no hazard exists with respect to possible head bolt failure.

During out-of-pile testing the maximum stress on the critical bolt will be increased to about 22,000 psi due to the reduced pressure of the external water. This stress is also well below the endurance limit.

A structural failure of this sort, even if it could occur, would result in a sudden increase in error signal and automatic stopping of the test with no more consequences than those described in the following section for ring seal failure.

3.8.1.2 Ring Seal (108-1063-1) Failure

The polyurethane seal (Shore Durometer A-70), between the head assembly and the test loop bulkhead, seats in a bulkhead groove approximately 4.9 inches in diameter. Because of the low relative stiffness of the seal, and the fact that its volume is less than that of the groove, nearly all of the prestress tensile load on the bolts is balanced by compressive loading of the cylindrical section of the head assembly.

The analysis given in Section 3.8.1.1 shows that during in-pile testing only about half of the compressive stress on the cylindrical section of the head assembly is relieved in the critical area when the maximum compressive load (3500 pounds) is applied to the specimen. Therefore, there is no danger of the contacting surfaces separating from the seal to cause a leak of water into the helium or helium into the water.

The polyurethane seal is replaced after each test so that the conservatively estimated maximum gamma dose it will receive during low-cycle fatigue testing in-pile (approximately 14 hours) is 4.3×10^4 ergs/gm (C). This is only about 1/4 the value allowable for this material even under dynamic loading conditions (ref. 8) so that no hazard should result from radiation damage to the seal, particularly since it is always nearly entirely enclosed by the contacting surfaces.

Out-of-pile testing does not give as great a margin of safety with respect to separation of the contacting surfaces because of the reduced external water pressure. But any leak under this condition will be immediately detectable and will not constitute a hazard to the reactor operation or even to the integrity of the test loop. If necessary, the pre-stress on the bolts can be increased to 21,600 psi each. Calculations indicate that this would more than compensate for the eccentric reduction in compressive load on the head assembly and would still not impose more than the endurance limit on the critical bolt.

The consequences of a seal failure are essentially the same as those for system rupture. A postulated sequence of events following seal failure would be as follows:

1) Seal fails.

2) Water freezes in head assembly.

3) Rupture disc relieves system at 75 psi.

4) Helium pressure drops.

5) Refrigeration system shuts down.

3.8.1.3 Head Assembly End Cap Failure

Exhaustive calculations have indicated that the load carrying member which exhibits the greatest stress is the test loop head assembly end cap.

With 3500 pounds maximum load on the specimen, the maximum stress in the end cap is 40,400 psi. This stress is well below the ultimate strength and only a little above the yield strength for 304 Stainless Steel. The localized yielding which would occur would not result in failure or even serious permanent deformation.

Consideration of the cyclic loading reveals that even the highest stresses in the end cap are well below the limits for 10^7 cycles. The highest ratio of cyclic stress to the limiting stress at the determined mean stress is 0.76.

A fatigue failure in this case would not result in a hazard since the only effect would be to break the vacuum in the head assembly (detectable immediately in the refrigeration system performance), or, at the most, to cause the automatic stopping of a test.

4 TEST PROCEDURES

The test procedures discussed in the following sections are required for the acquisition of data under the carefully controlled test program environmental conditions and the reduction, analyses and interpretation of the data thus generated. Brief discussions of test specimen designs, flux mapping, tensile test methods, fatigue test methods, and post-exposure structural studies follow.

4.1 TEST SPECIMEN DESIGN

The test specimens used in this program are miniaturized due to various restrictions on the test equipment imposed by the nuclear cryogenic environment. Two specimen designs, one for the tensile test program and one for the fatigue test program, are required.

The tensile specimen, shown in figure 4 and discussed in detail in reference 5, represents a miniaturization of the standard ASTM E-8 specimen (ref. 3). It is essentially a cylindrical tensile coupon, approximately two inches overall length, with threaded ends. The specimen gage length is 0.5 inch with a nominal diameter of 0.125 inch at the mid-point in the gage length, which conforms to the standard 4:1 gage length to diameter ratio. There is a slight taper to the mid-point of the gage length to insure fracture in that area.

The fatigue specimen design under consideration is shown in figure 5. Fatigue specimen design is not as standardized as tensile specimen design and the fatigue specimen to be used in this program will represent a departure from any commonly used design. However, the specimen geometric configuration is similar to that used by other investigators, such as Coffin (ref. 4). This will allow some degree of comparison between this data and data from other laboratories.

4.2 FLUX MAPPING

Accurate knowledge of the fast flux available in HB-2, both spectral shape and level, is necessary to determine the irradiation exposure required to provide the desired integrated flux for each specimen.

The fast flux was measured at various reactor operational parameters during the preceding reporting period (ref. 6) using fast neutron threshold foils (table 1). The results of these measurements are reported in detail in reference 6 and shown in figure 6.

A meeting of NASA and Lockheed personnel was held during an earlier reporting period for a discussion of the flux mapping activities. It was concluded that there was no significant change in flux level or spectral shape since the conclusion of the screening program. The flux curves used in the earlier program (ref. 1 and ref. 6) are still in use as the basis of exposure calculations.

4.3 TENSILE TEST METHODS

Tensile testing requires the measurement and recording of several data for post-testing evaluation. These data include:

- Measurement and recording of the load on the specimen continuously from the initial application until specimen failure.
- Measurement and recording of the elongation of the specimen continuously from initial application of the load until a point after the total elongation represents more than 0.2 percent permanent strain.
- Measurement of specimen temperature throughout irradiation and testing.
- Measurement of elongation (a measure of total permanent strain) and reduction of area (a measure of non-uniform strain) on failed specimens as a post-irradiation examination.

The test methods required to provide accurate records of these parameters have been discussed in some detail in a previous report (ref. 5). A brief summary of these methods will be included in the following section, with a more detailed discussion of the specimen temperature control development work conducted during this reporting period.

4.3.1 Load-Strain Measurement and Recording, Data Reduction, Ductility Measurements

Load measurements are monitored with a ring type dynamometer, using a linear variable differential transformer (LVDT) to measure the ring deflection resulting from the applied load. Elongation is measured using an extensometer in which a LVDT measures the incremental separation between two knife edges initially 0.50 inch apart on the gage length of the specimen.

For load-elongation recording, the monitoring instruments convert the load or elongation into electrical signals, of which the strength is a function of the magnitude of the measured parameter. The electrical impulse from each of these instruments is amplified and plotted automatically by an X-Y recorder. Load appears as the Y plot, elongation as the X plot and the resultant load-elongation curves are recorded on graph paper as a permanent record of these test data. The extensometer is capable of measuring only about 0.010 inch elongation with reliable accuracy. After this limit of approximately two percent total strain has been reached, the recorder is switched to a load-time plot traveling at a rate of 0.02 in/sec.

The load-elongation curve developed during testing on the X-Y recorder and the initial specimen dimensions provide data for the determination of the ultimate tensile strength (F_{tu}) and the tensile yield strength (F_{ty}). The modulus of elasticity may be approximated from these curves, but an exact determination of this value is unobtainable due to the method of extensometer installation imposed by the necessity of using remote handling techniques.

Elongation and reduction of area values are obtained by fitting the broken specimens together and measuring the fractured gage length and minimum diameter by means of a micrometer stage and hair line apparatus accurate to $\pm$ 0.0001 inch. These values are reported as the change in magnitude from original specimen dimensions expressed as a percentage of the original value.

All of these methods conform to the requirements of ASTM Specification E-8 (ref. 3), with an extensometer installation classification of B-2 under ASTM Specification E-83 (ref. 3).

4.3.2 Specimen Temperature Control

Test specimen temperature control is required for three different test conditions: (1) expose and fracture at specified temperature without intervening warm-up; (2) expose at 30°R followed by warming to and fracture at higher temperature; and (3) expose at 30°R, anneal at a higher temperature and fracture at 30°R.

The direct measurement of these temperatures using thermocouples or other temperature measuring transducers was not considered practicable when performing a series of these tests (ref. 1). An alternate method of establishing the temperature at the specimen was incorporated into the refrigerator. This involves measurement of the temperature at the manifold inlet and return using platinum resistance type thermometers. These temperature measurements together with the return manifold sensor temperature establish the operational characteristics of the refrigerator permitting the determination of performance parameters which are related to the specimen temperature.

The technique used consisted of calibration of three copper-constantan thermocouples attached to a Titanium 6Al-4V test specimen against a NBS calibrated platinum resistance thermometer and using this instrumented specimen as a working standard to establish refrigeration system operating parameters required for the maintenance of the desired specimen temperature both in-pile and out-of-pile. This activity is reported in detail in reference 5 and reference 6 and the important results are summarized in tables 2 and 3.

4.4 FATIGUE TEST METHODS

After determination of a suitable test specimen (see section 4.1), low-cycle fatigue characteristics of selected materials will be studied. The test procedure will consist of applying a predetermined stress load and cyclic rate of 15 cpm for 10,000 cycles unless the test is interrupted before this point by specimen failure.

Procedures for the fatigue test program have been approved by NASA and in-pile fatigue testing will be inaugurated in the next reporting period.

4.5 STRUCTURAL STUDIES

Structural studies are to be performed with the aid of optical microscopy, electron microscopy, and X-ray diffraction. Procedures for these methods are being developed in cooperation with NASA Plum Brook Reactor Facility personnel.

5 TEST PROGRAM

The materials, pure aluminum, titanium and titanium alloys, to be tested during this program were selected on the basis of their potential usefulness in nuclear-cryogenic space hardware and their ability to yield fundamental information in terms of basic mechanisms occurring in metals and alloys during and following fast neutron irradiation at cryogenic temperatures. The scope of the test program, including the basis for material selection, has been previously reported (ref. 5 and ref. 6) and consists of the following major items of investigation:

- Effects of cryogenic irradiation and annealing on tensile properties of Aluminum 1099-H14.
- Effects of irradiation at 30°R on tensile properties of titanium and titanium alloys.
- Effects of irradiation on low-cyclic rate fatigue properties of titanium and titanium alloys.

All test specimens used in the program are fabricated from materials manufactured using extraordinary precautions and provided with complete chemical and metallurgical pedigrees. A summary of the pedigree information is given in tables 4 and 5.

5.1 EFFECTS OF CRYOGENIC IRRADIATION AND ANNEALING ON ALUMINUM 1099-H14

Aluminum 1099 is a high purity (99.99%) aluminum and, although it is of little value as a structural material, was selected for study because it has exhibited very large effects due to irradiation at 30°R (ref. 1). The material also exhibited some annealing effects as well as effects due to deformation prior to irradiation. This combination of effects offers a good opportunity for study of irradiation-cryogenic mechanisms at a relatively low level of integrated neutron flux.

The testing of Aluminum 1099, as set forth in table 6, consists of out-of-pile control tests and in-pile tests for the following four studies:

- Effects of irradiation at 30°R
- Effects of irradiation temperature
- Effects of annealing and test temperature following irradiation
- Effects of annealing

All tensile testing was completed during this reporting period. Structural studies in the hot metallurgical laboratory will be initiated during the next reporting period.

5.1.1 Effects of Test Temperature, No Irradiation, Control Tests

Aluminum 1099-H14 was tested at 30°R, 140°R, 320°R, and 540°R without irradiation to obtain control test data for the nuclear cryogenic irradiation and annealing studies. These data are given in table 7, along with pertinent data from the previous screening program (ref. 1). The magnitude of the cryogenic effects on the tensile properties are shown in the family of curves plotted in figure 7. Figure 8 shows a family of load-elongation curves for the various test temperatures.

Extra test values were obtained for control purposes at the various temperatures to determine if there were any possible systematic effects of temperature changes prior to testing. If existant, such changes could be attributed to differential thermal contraction in the specimen loading components of the test loop and would have to be considered in the evaluation of the annealing data taken with the test loop components subjected to the same temperature changes. It should be noted that special precautions during insertion of the specimen and preparation for testing are meant to exclude this possibility. If observed at all, such effects would be observed in the yield strength values. Evaluation of the data indicates that in nearly all cases, there are no statistically significant differences (at the 90% confidence level).

There is a significant difference, small compared with irradiation effects, at 320°R but this difference is attributable to location in the stock from which the specimens were taken. The test specimens are numbered according to the location from which they were taken in the plate stock and are generally chosen at random for a particular test condition. This results in effects due to variations in the material and tensile properties within the stock being averaged out. However, in this particular case there was an error in the choice of specimens with the resulting nonrandom location which could easily account for the small but statistically significant difference between the yield strength values from the two groups of tests at 320°R. This conclusion is confirmed by differences in ultimate strength and ductility values, small compared with test temperature effects, which can also be attributable to location in the stock.

Although there are no significant differences between the various groups of tests at 30°R, there is a significant difference between these values as a group obtained in the current program and the values obtained at the same temperature in the screening program (ref. 1). These differences have to be attributed to differences in work hardening during fabrication because of the lack of similar differences in the ultimate strength and ductility values. Although little work has been done at extremely low temperatures on this material, test data from other laboratories (ref. 9) indicates the probability of a cold-work dependent divergence of F_{ty} at temperatures below 140°R for commercially pure aluminum (Aluminum 1100).

Because the noted differences can be attributed to stock variation and fabrication variables rather than to differences in test conditions, the means and the ranges of all the values obtained at the particular temperatures are being used as control data.

Examination of the family of curves shown in figure 7 shows that the F_{ty} is relatively insensitive to temperature variation while the F_{tu} is strongly temperature dependent, particularly below 140°R. This, naturally, produces a profound effect on the F_{ty}/F_{tu} ratio. Also worthy of note is the rather sharp drop in reduction of area occurring below 140°R. The relatively high reduction of area to elongation ratio at temperatures above 140°R indicate a large degree of necking down during late plastic behavior; a value near unity for this ratio at lower temperatures is indicative of uniform plastic strain.

Although the range of the data for the F_{ty} obscures the magnitude of a specific effect, the overall relationship of the several tensile test parameters justifies the general validity of the difference of cryogenic strain mechanism discussed in the summary report of the screening program (ref. 1).

5.1.2 Effects of Irradiation at 30°R

This study is to determine the effects of neutron irradiations up to $3 \times 10^{17} n/cm^2$ ($E > 0.5$ MeV) at 30°R on Aluminum 1099-H14. The specimens are held at 30°R throughout irradiation and tensile testing. Test results are given in table 8 and shown graphically in figure 9. A family of load-elongation curves for this material at the several irradiation levels is shown in figure 10.

Examination of figure 9 shows that the net change in the strength and ductility functions is dependent on irradiation level, with no evidence of any saturation effects at these irradiation levels. Note also the effect on the F_{ty}/F_{tu} ratio which is clearly governed by the level of irradiation. At $3 \times 10^{17} n/cm^2$ ($E > 0.5$ MeV), the cryogenic depression of this ratio, evident in the unirradiated control specimen tested at 30°R (see fig. 7), has virtually been eliminated by interaction between neutrons and lattice atoms. In this instance, the irradiation effect seems to resemble the effect of cold working on the intercrystalline critical shear stress.

5.1.3 Effects of Irradiation Temperature

This phase of the testing program is for the purpose of studying the magnitude of the irradiation effect as a function of irradiation temperature. The specimens are irradiated to $1 \times 10^{17} n/cm^2$ ($E > 0.5$ MeV) at 140°R, 320°R, or 540°R, then fractured at the irradiation temperature. Test results are given in table 9 and shown in figure 11.

Comparison of figure 11 with figure 7, the cryogenic effects on non-irradiated Aluminum 1099-H14, shows a marked similarity in geometric form in all functions except the yield strength (F_{ty}) and, naturally, the F_{ty}/F_{tu} ratio. The effect of irradiation at near room temperatures is slight at levels to $10^{17} n/cm^2$ ($E > 0.5$ MeV); the effect of cryogenic irradiation is observable particularly in the changes induced in the yield strength (Fty) and, obviously, the F_{ty}/F_{tu} ratio.

5.1.4 Effects of Annealing and Test Temperature Following Irradiation

This study is to determine the magnitude of irradiation effects remaining at various temperatures following irradiation at 30°R. The specimens are irradiated to $1 \times 10^{17} n/cm^2$ ($E > 0.5$ MeV) at 30°R and then warmed to a higher temperature

and annealed at that temperature for an hour and tested at that temperature. The test results are shown in table 10 and figure 12.

Comparison of figure 12 to the data presented in figure 11 indicates that the net effects of annealing and testing at temperatures above the irradiation temperature of 30°R is quite similar to those resulting from irradiation at the "annealing" temperature. Annealing and testing at near room temperature results in essentially complete removal of irradiation induced effects. Annealing and testing at lower temperatures leaves a significant irradiation induced effect on the F_{ty} and the F_{tu}/F_{ty} ratio, with a lesser residual effect on the F_{tu}.

5.1.5 Effects of Annealing Following Irradiation

This study is to determine the magnitude of recovery at various temperatures of irradiation effects occurring at 30°R. The specimens are irradiated to 1×10^{17} n/cm^2 ($E > 0.5$ MeV) at 30°R and then warmed to a higher temperature and annealed at that temperature for an hour. They are then cooled to and stabilized at 30°R and tested. The data obtained are presented in table 11 and figure 13.

Since a direct comparison with the annealing studies discussed in 5.1.4 is desirable, a sumation of test data in both sections is given in figure 14 with the data reduced to a common set of ordinates. Due to the large variation of the magnitudes in the individual function between the different test conditions, this plot is based on test value ratios (V) as a function of temperature. The test value ratio was determined as follows:

- For anneal at T and test at 30°R

$$V_{30} = \frac{F_t \text{ @ } 30°R \text{ after irradiation to } 10^{17} \text{ at } 30°R \text{ and 1 hr anneal at T}}{F_t \text{ @ } 30°R, \text{ no irradiation}}$$

- For anneal and test at T

$$V_T = \frac{F_t \text{ @ T after irradiation at } 30°R \text{ to } 10^{17}, \text{ and 1 hr anneal at T}}{F_t \text{ @ T, no irradiation}}$$

where V = TEST VALUE RATIO
T = Annealing temperature
F_t = Tensile Test Value obtained at described condition

In the interest of clarity, only the F_{tu} and the F_{ty} have been included in the plot shown in figure 14.

Examination of figure 14 shows that an effect of irradiation at 30°R on F_{ty} appears to anneal out if tested at higher temperatures but is still observable through testing at 30°R following the annealing.

5.1.6 Discussion

Examination of the several tables and figures referenced in the preceeding sections (5.1.1 through 5.1.5) reveals an inter-relationship of the test data generated under varying conditions for Aluminum 1099-H14.

Examination of the data presented in table 7, and plotted in figure 7, shows the significant effect of cryogenic environments, without irradiation, on the work hardened aluminum. Although the F_{ty} is largely a temperature independent function, both the F_{tu} and the elongation in 0.5 inch are markedly increased by reduction in temperature. At 30°R, the material exhibits essentially uniform strain, as shown by the close approach of the elongation in 0.5 inch and the reduction of area curves in figure 7. The F_{ty}/F_{tu} ratio drops from near unity, at room temperature, to 0.32 at 30°R. The over-all effect on mechanical properties of cryogenic exposure would seem to resemble annealing; the ductility parameters for Aluminum 1099-H14 at 30°R are similar to those of 1099-0 at room temperature and the strength functions have a similar relationship, with the 30°R values showing a cryogenicly induced increase in magnitude by about a factor of three. As figure 7 shows, these effects are slight above about 300°R, moderate in the region of 140°R (Liquid Nitrogen temperature) and quite marked at lower temperatures.

The effect of fast neutron irradiation at 30°R, shown by the data presented in table 8 and plotted in figure 9, appears similar to that of the initial cold work which provided the H14 temper. Even at quite low irradiation exposures, 5×10^{15} n/cm^2 ($E > 0.5$ MeV), the hardening effect is observable through a slight increase in the F_{ty} and the F_{ty}/F_{tu} ratio. The net increases in both F_{ty} and F_{tu} are essentially linear functions or irradiation level to 3×10^{17} n/cm^2 ($E > 0.5$ MeV); however, the greater slope of the F_{ty} shown in figure 9 indicates an irradiation hardening effect similar to cold work. The increase in F_{ty}/F_{tu} ratio as a function of irradiation level is shown in the same figure. The inter-relationship of the mechanical properties at 30°R with increasing irradiation levels approachs that of the unirradiated material at room temperature with but two notable exceptions: the much greater tendency for necking-down immediately prior to failure (shown by

the reduction of area) and the lower fracture stress for the unirradiated material. Since the data required to provide a correction for the tri-axial loading conditions during fracture of the unirradiated material are not available these fracture stress values are likely to be in error (ref. 10). The greater instability in tension of the unirradiated material might be attributed to a difference in the nature of void nucleation sites between irradiated and unirradiated aluminum. Grain boundry dislocation pile-ups large enough to produce cavity dislocations would appear more probable as a source of fracture initiation in irradiated material, the failure would be more likely to originate at foreign particle sites in the unirradiated stock. Structural studies will be made to explore this possibility. However, since the formation of a neck under tensile stresses occurs after the maximum load during deformation, the engineering importance of this difference in behavior seems limited.

A rapid evaluation of the effects of test temperature of Aluminum 1099-H14 with various irradiation histories can be made by comparing figures 7, 11 and 12. The data plotted in figure 11, presented in table 9, was obtained from specimens irradiated to 10^{17} n/cm^2 (E > 0.5 MeV) at the test temperature; that plotted in figure 12, presented in table 10, from specimens irradiated to 10^{17} n/cm^2 (E > 0.5 MeV) at 30°R and held at the test temperature for one hour prior to testing. Comparison of figures 11 and 12 shows no essential difference in the data; apparently the irradiation temperature is not significant if the specimens are annealed and tested at temperatures at or above the irradiation temperature. At temperatures above 320°R, the curves shown in figures 11 and 12 are similar to those of figure 7. The effect of irradiation to 10^{17} n/cm^2 (E > 0.5 MeV) at and above this temperature is negligable. Below that temperature, the effect of the level of irradiation on the F_{ty} is pronounced and the F_{ty}/F_{tu} ratio remains reasonably constant and the degree of specimen necking is reduced.

In examination of figure 14, a comparison of the mitigation of the effects of irradiation to 10^{17} n/cm^2 (E > 0.5 MeV) at 30°R through annealing as measured at the annealing temperature and at the irradiation temperature, shows that a marked residual irradiation effect is observable by post-annealing testing at 30°R which is not discernable through testing at annealing temperatures.

5.2 EFFECTS OF IRRADIATION AT 30°R ON TENSILE PROPERTIES OF TITANIUM AND TITANIUM ALLOYS

The titanium alloys of primary alpha structure usually exhibit good cryogenic properties due to the hexagonal close-packed structure of this phase. They have a high modulus of rigidity and a high strength-weight ratio, which is comparable with the best aluminum alloys. Also, they have allowable working temperatures which are higher than the aluminum alloys. This makes them more suitable for rocket components, initially at cryogenic temperatures, which may see elevated temperatures during rocket firing.

The tensile testing phase of the program, as set forth in table 12, consists of three investigations:

- Effects of irradiation at 30°R on commercially pure titanium (Ti-55A).
- Effects of interstitial content in Ti-5Al-2.5 Sn on changes due to irradiation at 30°R.
- Effects of initial heat treatment of Ti-6Al-4V on changes due to irradiation at 30°R.

Out-of-pile test data and in-pile test data for irradiations to 1×10^{17} n/cm^2 ($E > 0.5$ MeV) were obtained in the screening program (ref. 1). The mechanical testing phase of the in-pile portion of the present program is nearing completion. All tests, shown in table 12, for Ti-55A, Ti-5Al-2.5 Sn (ELI), and Ti-6Al-4V (Annealed) have now been completed. Structural studies will be initiated during the next reporting period.

5.2.1 Effects of Irradiation At 30°R on Titanium 55A

Titanium 55A, although of only moderate strength, has good forming characteristics and meets the requirements for some nuclear rocket applications; however, it was selected for study in this program primarily because it is essentially commercially pure elemental titanium and may yield important fundamental information. It has exhibited a small but measurable increase in yield strength due to fast neutron irradiation of 10^{17} n/cm^2 ($E > 0.5$ MeV) at 30°R (ref. 1).

This phase of the test program was completed in a previous period and reported in reference 6. The test results are repeated in table 13 and plotted as a function of integrated neutron flux at 30°R in figure 15. Figure 16 shows typical load-elongation curves for the various irradiation levels included in the testing phase of the investigation.

The data plotted in figure 15 show that there is a direct dependence of F_{tu} and F_{ty} on irradiation level (to 10^{18} n/cm^2 (E > 0.5 MeV)) accompanied by a significant but not critical reduction in ductility parameters. No degradation of any mechanical property of sufficient magnitude to compromise engineering integrity after exposures to 10^{18} n/cm^2 (E > 0.5 MeV) was observed.

Titanium 55A is essentially a polycrystalline titanium of commercial purity. This material was tested in the annealed condition, but with standard interstitial content; therefore, the population of "foreign" substitutional solute atoms should be small but the number and distribution of interstitial atoms should be similar to the interstitial populations in alloyed materials. Since alpha titanium is a hexagonal close packed lattice material, slip might be expected to be fairly laminar -- particularly with a relatively small population of substitutional atoms. The presence of interstitials might be expected to increase turbulence of the flow during slip. Since the reported F_{ty} is based on 0.2% offset rather than on divergence from Hookes Law, the relatively low (for titanium alloys) F_{ty}/F_{tu} ratio of about 0.7 at 30°R, both unirradiated and at 1×10^{17}, indicate a rather laminar behavior; the increase of this parameter to 0.75 at 6×10^{17} and 0.78 at 1×10^{18} indicates an increase in turbulence resultant from lattice imperfections induced by increased irradiation levels.

5.2.2 Effects of Interstitial Content in Ti-5Al-2.5 Sn On Changes Due To Irradiation At 30°R

Titanium - 5% Al - 2.5% Sn is a fairly high strength alpha phase alloy ($F_{tu} \approx 120$ Ksi at room temperature). It is now commercially available in the extra low interstitial grade (less than 0.125% interstitials, and designated ELI) and possibly would be specified in this grade by designers for use in shells, pressure vessels and pump parts of nuclear rockets. However, recent nuclear cryogenic tests to 10^{17} n/cm^2 (E > 0.5 MeV) at 30°R, (ref. 1), indicate that the ultimate strength of the ELI material is adversely effected by the neutron irradiation. It is conceivable that higher irradiations might cause adverse effects on various properties, including fatigue strength, which would negate any inherent advantages of the ELI material.

In addition, tensile testing of both grades of this alloy might yield fundamental information on the general role of interstitials in nuclear cryogenic processes occurring in all metals and alloys.

During this reporting period in-pile tensile testing following irradiations of 1×10^{18} n/cm^2 (E > 0.5 MeV) at 30°R was completed on this material in the extra low interstitial (ELI) grade. Test results are presented in table 14 along with data obtained previously (ref. 1). These test data are presented graphically in figure 17. Load-elongation curves are not published since, due to the high F_{ty}/F_{tu} ratio and limited ductility of this alloy, they provide no information which can not be observed by inspection of the test data. Since no specimens were tested at irradiation levels between 10^{17} and 10^{18}, no effort to determine the shape of the intervening curve could be made and a linear plot is presented in figure 17.

Comparison of figure 17 with figure 15 shows essentially similar behavior for Ti-5Al-2.5 Sn (ELI) and commercially pure Titanium. The higher unirradiated F_{ty}/F_{tu} ratio for the 5 Al-2.5 Sn alloy, attributable to the alloying content and indicative of a rather turbulent type of flow during slip, is observable at both irradiation levels. Further evaluation of the effect of interstitials will be deferred until data for Titanium 5 Al-2 1/2 Sn (STD) is available.

5.2.3 Effects of Initial Heat Treatment of Ti-6Al-4V On Changes Due To Irradiation At 30°R

Titanium - 6% Al - 4% V is an alpha-beta alloy in which the beta phase is meta-stable in the annealed condition and largely transformed to alpha by aging. The ultimate strength of the aged materials is about 170 Ksi at room temperature with favorable cryogenic characteristics and it is very likely to be specified for shells and pressure vessels in space hardware. Irradiation to 10^{17} n/cm^2 (E > 0.5 MeV) at 30°R causes measurable increases in the strength of the aged material but not the annealed material. Higher irradiations at the same temperature may confirm this effect and may possibly yield fundamental information regarding the effects of nuclear irradiation on precipitation processes. Such effects are still not very well understood although they are of wide general interest to both basic researchers and applications people.

During this reporting period, the in-pile tensile test program, table 12, was completed for the annealed material. Test results are presented, along with data previously obtained (ref. 1), in table 16. The test data are presented

graphically in figure 18, where straight lines are used, rather than curves, due to the lack of data between 10^{17} and 10^{18} n/cm^2 (E > 0.5 MeV). Load-elongation curves are not published since, due to the high F_{ty}/F_{tu} ratio and limited ductility of this alloy, they provide no information which can not be observed by inspection of the test data.

Comparison of figures 15, 17 and 19 shows the annealed Ti-6Al-4V to change in a manner similar to the commercially pure material and the 5 Al-2.5 Sn (ELI) alloy.

No further evaluation of test results will be made until test data from the aged material is available for comparison.

5.3 LOW-CYCLE FATIGUE TESTING

The low-cycle fatigue testing phase of the program is shown in table 18. The test materials to be used are the same as those used in the titanium and titanium alloys portion of the tensile testing program.

To date, only a minimum number of tests have been conducted, and these only out-of-pile on Titanium 55A at 540°R and 30°R. These tests were largely to verify equipment operation and, although reasonably self consistant, considering the scatter normal in fatigue data, results are not sufficient to be presented at this time.

With the tensile testing phase of the program nearing completion, a larger proportion of the over all effort is now going into fatigue testing and some results of this testing will be presented in the next quarterly report.

6 CONCLUSIONS

The mechanical properties of Aluminum 1099-H14 under a wide variety of nuclear cryogenic test conditions have been determined during this reporting period. The interrelationship of the test data can be examined to arrive at certain important conclusions with regard to both similarities and differences in the data from various test conditions.

The most prominent observable effect of cryogenic temperatures on Aluminum 1099-H14 in the absence of irradiation is in a reduction of the yield to tensile ratio (F_{ty}/F_{tu}) with decreasing temperatures. This is accompanied by a sharp increase in the uniform strain, as constrasted with necking down, occurring during plastic deformation. The notable increase in elongation accompanying the reduction of F_{ty} at cryogenic temperatures (unirradiated) indicates a mitigation of the effect, at room temperature, due to cold work in the H14 material. The reduction of area values confirm this trend, although this parameter usually shows a greater range of values than the other functions, since it is the most structure sensitive of those values measured in tensile testing.

The effect of fast neutron bombardment on Aluminum 1099-H14 at 30°R is to increase the strength values and reduce the ductility values. There is a tendency for the F_{ty}/F_{tu} ratio and the elongation to assume their approximate levels for the unirradiated material tested at room temperature. The data shows that this recovery is primarily due to an increase in the F_{ty} and the hardening mechanism resulting from the irradiation appears to resemble that resulting from cold work.

Comparison of the F_{ty}/F_{tu} and elongation values for Aluminum 1099-H14 at room temperature, unirradiated, with those at 30°R after irradiation (at 30°R) show a remarkable similarity. Although there is an increase in the strength values (F_{tu} and F_{ty}) by approximately a factor of 3, accompanied by a decrease of about 50 percent in the reduction of area, the elongations are essentially the same for the two test conditions. This indicates that any combined nuclear-cryogenic induced embrittlement accompanying the increase in strength values effects only the necking-down portion of the plastic behavior. The only instance in which the behavior of the irradiated material at 30°R resembles that of the unirradiated material at 30°R more closely than that of the unirradiated material at room temperature is in the relative uniformity of plastic strain.

Thus, in a very important respect, the cryogenic (unirradiated) induced mitigation of the effects of cold work in Aluminum 1099 in the H14 condition can be overcome by neutron irradiation.

A comparison of the data from irradiating Aluminum 1099-H14 and testing at various temperatures to that from irradiating at 30°R and then annealing and testing at various temperatures indicates an essential similarity, with no significant differences at particular test temperatures between the data from the two test conditions.

Comparison of the data indicates that in the normal temperature range (above about 350°R) the effects of irradiation to 10^{17} n/cm^2 (E > 0.5 MeV) are slight and the effects of irradiation at cryogenic temperatures tend to anneal out if the material is warmed to room temperature. At lower temperatures the effects persist to a much greater degree. At temperatures below 320°R, the F_{ty}/F_{tu} ratio remains about constant with irradiation or annealing temperature while necking down during plastic deformation is reduced, accompanied by an irradiation induced increase in the strength values. This confirms the similarity of irradiation effects and work-hardening.

To facilitate an analysis of annealing of nuclear cryogenic effects in Aluminum 1099-H14, the data was reduced to ratios of strengths at test conditions to strengths without irradiation at corresponding test temperatures. The results show that the effects induced by irradiation to 10^{17} n/cm^2 (E > 0.5 MeV) at 30°R appear to be completely annealed out when tested at 540°R and essentially annealed when tested at much lower temperatures. However, testing the material at 30°R following annealing at various temperatures, including 540°R, indicates considerable residual irradiation effects. The difference in behavior is, not unexpectedly, more pronounced in the F_{ty} than in F_{tu} values. This effect is even more pronounced in the increase in the uniform strain component of the plastic deformation with increasing annealing temperatures.

Conclusions based on the still incomplete test data for the titanium and titanium alloys are not warranted at this time.

7 REFERENCES

Reference	
1	Lockheed Nuclear Products: Effect of Nuclear Radiation on Materials at Cryogenic Temperatures. NASA CR-54881, 1966.
2	Lockheed Nuclear Products: Modification and Major Overhaul of Cryogenic Irradiation Facility at Plum Brook Reactor Facility. NASA CR-54770.
3	Anon: ASTM Standards, The American Society For Testing Materials, 1958, Part 3.
4	Coffin, L.F. Jr.; and Tavernelli, J.F.: The Cyclic Straining and Fatigue of Metals. Trans. Met. Soc. AIME, Vol 215, Oct. 1959, pp 794-807.
5	Lockheed Nuclear Products: Effect of Nuclear Radiation on Materials at Cryogenic Temperatures. NASA CR-54787, November 1965.
6	Lockheed Nuclear Products: Effect of Nuclear Radiation on Materials at Cryogenic Temperatures. NASA CR-54904, February 1966.
7	Lockheed Nuclear Products: Effect of Nuclear Radiation on Materials at Cryogenic Temperatures. NASA CR-54976, May 1966.
8	King, R.W.; Broadway, N.J.; and Palinchak, S.: The Effect of Nuclear Radiation on Elastomeric Components and Materials. REIC Report No 21.

9 Cryogenic Materials Data Handbook, Technical Document Report No. ML-TDR-64-280, August 1964.

10 Dieter, George E. Jr.: Mechanical Metallurgy, McGraw-Hill Book Co., Inc., 1961.

8 TABLES

TABLE 1 FLUX MAPPING FOILS

Type of Foil	Nuclear Reaction	Threshold Energy, E_T (Mev)	Cross Section ($\times 10^{-24}$ cm^2)
Indium	$In^{115}(n,n')In^{115\,m}$	0.45	0.20
Neptunium	$Np^{237}(n,f)\,Ba^{140}$	0.75	1.52
Uranium	$U^{238}(n,f)\,Ba^{140}$	1.45	0.54
Sulfur	$S^{32}(n,p)\,P32$	2.9	0.284
Nickel	$Ni^{58}(n,p)Co^{58}$	5.0	1.67
Magnesium	$Mg^{24}(n,p)Na^{24}$	6.3	0.0715
Aluminum	$Al^{27}(n,\alpha)\,Na^{24}$	8.6	0.23

TABLE 2 IN-PILE TEMPERATURE CORRELATION DATA

Test Run	Specimen Temperatures (°R) Fwd.	Mid.	Aft	Refrig. Temperatures (°R) Loop Inlet	Loop Return	Return Manifold	Heater Loads Main (watts)	Trim (watts)	Expansion Engine Pressure Ratio	Speed (RPM)
(30°R)										
1	30.4	29.9	30.3	29.1	32.3	32.3	200	40	6.1:1	325
2	30.7	30.3	30.6	29.0	32.6	32.6	200	25	6.0:1	320
3	30.4	29.8	30.2	29.1	32.5	32.5	200	30	6.1:1	320
(70°R)										
1	70.2	70.1	70.1	67.8	76.6	76.6	1200	20	6.1:1	325
2	70.4	70.3	70.1	67.3	77.1	77.0	1100	35	6.0:1	325
(140°R)										
1	140.0	139.6	139.8	136.2	150.5	150.0	1050	25	5.9:1	250
2	141.0	140.5	140.9	136.0	150.0	149.6	1100	5	6.0:1	250
(320°R)										
1	322.0	321.0	320.7	317.8	332.0	332.2	1300	70	6.0:1	250
2	320.5	319.6	320.1	318.2	331.7	331.8	1300	25	6.0:1	260

TABLE 3 OUT-OF-PILE TEMPERATURE CORRELATION DATA

Test Run	Specimen Temperatures (°R)			Refrig. Temperatures (°R)			Heater Loads		Expansion Engine	
	Fwd.	Mid.	Aft	Loop Inlet	Loop Return	Return Manifold	Main (watts)	Trim (watts)	Pressure Ratio	Speed (RPM)
(30°R)										
1	30.2	30.1	30.3	29.5	31.0	31.2	350	20	6.1:1	300
2	29.6	29.4	29.7	29.7	31.3	31.4	400	60	6.2:1	290
3	29.8	29.3	29.5	29.2	30.5	30.5	400	10	6.1:1	280
(70°R)										
1	70.3	70.1	70.6	68.0	72.1	72.0	1350	10	6.0:1	280
2	70.1	69.9	70.4	68.0	72.2	72.0	1250	60	6.2:1	270
(140°R)										
1	140.2	140.1	140.4	138.0	142.0	142.0	1600	35	6.1:1	260
2	140.6	140.4	140.8	138.5	142.7	142.5	1550	60	6.2:1	260
(320°R)										
1	320.1	320.1	320.2	318.1	322.3	322.0	1700	55	6.0:1	260
2	320.8	320.9	321.0	319.1	323.5	323.1	1650	25	6.0:1	270

TABLE 4 MATERIAL COMPOSITION (PEDIGREE DATA)

ALLOY / Temper	Lockheed Code	Element Weight Percent Al	Cu	Fe	Si	Mn	Mg	Zn	Ni	Cr	Ti
Aluminum 1099 - H 14	8 Ba	99.99	0.003	0.001	0.001						

		Ti	C	Fe	Al	Sn	V	N_2	H_2	O_2
Titanium 55A Annealed	1 Aa	*	0.032	0.19				0.023	0.006	0.218
Ti-5Al-2.5 Sn (Std. I)	3 Aa	*	0.032	0.110	5.10	2.5		0.019	0.012	0.116
Ti-5Al-2.5 Sn (ELI) Annealed	8 Aa	*	0.033	0.028	5.43	2.41		0.011	0.0056	0.053
Ti-6Al-4V Annealed	2 Ac	*	0.010	0.170	5.95		4.00	0.022	0.006	0.065
Ti-6Al-4V Solution Treated and Aged	2 Aa	*	0.010	0.15	5.80		3.90	0.035	0.010	0.102

* Balance (by difference)

TABLE 5 MATERIAL PHYSICAL CHARACTERISTICS (PEDIGREE DATA)

Alloy / Temper	Lockheed Code	Form	Spec.	Vendor Code / Vendor Lot or Heat No.	F_{tu} (Ksi)	F_{ty} 0.2% offset (Ksi)	Elongation in 0.5 in (4D) (%)	Hardness	Grain Size ASTM No. (E112-58T)
Aluminum 1099 -H14	8 Ba	0.5" Plate	Vendor	199352 (1)	13.50*	12.90	20.5	Brinell	Not Measured
				199352	14.25**	13.95	19.5	26	
Titanium 55A Annealed	1 Aa	0.5" Round Bar	Mil-T-7993A Class II	(2) M-9186	70.5	60.5	35	Rockwell B 87	5
Ti-5Al-2.5 Sn (Std. I) Annealed	3 Aa	0.5" Round Bar	AMS-4910	(2) M-7888	131.0	127.0	22	Rockwell C 31-33	8
Ti-5Al-2.5 Sn (ELI) Annealed	8 Aa	0.5" Round Bar	Vendor 49021-1	(2) V-2402	119.3	101.2	17	Rockwell C 24.9	Not Measured
Ti-6Al-4V Annealed	2 Ac	0.5" Round Bar	Mil-T 9047C	(2) M8574	146.0	138.0	15.5	Rockwell C 30-33	Not Measured
Ti-6Al-4V Solution Treated And Aged	2 Aa	0.5" Round Bar	Mil-T 9047C	(2) M-9812	173.0	165.0	13	Rockwell C 33-36	Not Measured

* Longitudinal (orientation of test program specimens)
** Transverse

(1) Aluminum Company of America
(2) Titanium Metals Corporation of America

TABLE 6 SCOPE OF TEST PROGRAM FOR STUDYING THE EFFECTS OF CRYOGENIC IRRADIATION AND ANNEALING ON TENSILE PROPERTIES OF ALUMINUM 1099-H14

Material	Condition	Number Specimens	Exposure n/cm^2 (E>0.5 MeV)	Exposure Temperature (°R)(1) Exposure	Post-Exposure	Remarks (7)
1099 Al	-H14	3	5×10^{15}	30	--	
1099 Al	-H14	3	5×10^{16}	30	--	
1099 Al	-H14	3	1×10^{17}	30	--	(2)
1099 Al	-H14	3	3×10^{17}	30	--	
1099 Al	-H14	3	0	140	--	
1099 Al	-H14	3	1×10^{17}	140	--	
1099 Al	-H14	3	0	320	--	
1099 Al	-H14	3	1×10^{17}	320	--	
1099 Al	-H14	3	1×10^{17}	540	--	
1099 Al	-H14	3	0	30	140	(3)
1099 Al	-H14	3	1×10^{17}	30	140	(4)
1099 Al	-H14	3	0	30	320	(3)
1099 Al	-H14	3	1×10^{17}	30	320	(4)
1099 Al	-H14	3	0	30	540	(3)
1099 Al	-H14	3	1×10^{17}	30	540	(4)
1099 Al	-H14	3	0	30	140	(5)
1099 Al	-H14	3	1×10^{17}	30	140	(6)
1099 Al	-H14	3	0	30	320	(5)
1099 Al	-H14	3	1×10^{17}	30	320	(6)
1099 Al	-H14	3	0	30	540	(5)
1099 Al	-H14	3	1×10^{17}	30	540	(6)

(1). Data from tests at 30°R and 540°R without irradiation available from screening program (ref. 1).
(2). Data from one specimen for this condition available from screening program (ref. 1).
(3). Control specimen, to be stabilized at exposure temperature before stabilizing and testing at post-exposure temperature.
(4). To be stabilized at post-exposure temperature before testing at post-exposure temperature.
(5). Control specimen to be stabilized at exposure and post-exposure temperatures before stabilizing and testing at 30°R.
(6). Temperature to be reduced to and stabilized at 30°R before testing at 30°R.
(7). All tests completed at the end of this reporting period.

TABLE 7 TEST RESULTS, EFFECTS OF TEST TEMPERATURE, ALUMINUM 1099-H14 (NO IRRADIATION)

Specimen	Temp. (°R)	F_{tu} (Ksi)	F_{ty} 0.2% offset (Ksi)	F_{ty}/F_{tu}	Elongation in 0.5 in (4D) (%)	Reduction of Area (%)	Fracture Stress (Ksi)	Modulus(#) (10^3 Ksi)
Range of 5(a)	30	30.0-39.3	6.0-8.2	0.17-0.27	60-63	61-76	110-110	7-12
Mean of 5(a)	30	33.78	6.97	0.216	61.4	69.2	110.0	11
8 Ba 107	30 (1)	40.0	10.7	0.27	55	67	99	13
8 Ba 112	30 (1)	38.0	16.6	0.44	55	56	66	11
8 Ba 115	30 (1)	39.8	14.5	0.36	49	57	70	7
8 Ba 130	30 (2)	38.6	15.8	0.41	61	61	86	12
8 Ba 142	30 (2)	37.4	12.9	0.34	56	65	76	9
8 Ba 148	30 (2)	37.8	14.7	0.39	56	64	79	10
8 Ba 99	30 (3)	38.3	15.1	0.39	59	70	91	11
8 Ba 101	30 (3)	39.5	15.3	0.39	57	68	94	5
8 Ba 110	30 (3)	43.1	17.3	0.40	54	62	86	14
Mean of 14	30	37.25	12.00	0.319	57.9	65.4	92.6	10
8 Ba 136	140	21.5	14.0	0.65	48	78	41	8
8 Ba 138	140	21.0	13.1	0.62	48	78	41	4
8 Ba 139	140	21.1	13.9	0.66	46	82	54	6
8 Ba 125	140 (1)	22.9	13.9	0.61	46	73	48	8
8 Ba 144	140 (1)	22.8	15.1	0.66	47*	83*	-	4
8 Ba 154	140 (1)	21.1	13.9	0.66	47	83	61	19
Mean of 6	140	21.73	13.98	0.643	47.0	79.5	49.0	8

TABLE 7 (CONTINUED)

Specimen	Temp. (°R)	F_{tu} (Ksi)	F_{ty} 0.2% offset (Ksi)	F_{ty} / F_{tu}	Elongation in 0.5 in (4D) (%)	Reduction of Area (%)	Fracture Stress (Ksi)	Modulus(#) (10^3 Ksi)
8 Ba 149	320	13.9	11.9	0.86	28	82	46	8
8 Ba 150	320	13.3	11.5	0.86	27	84	41	6
8 Ba 151	320	14.4	12.7	0.88	28	81	42	10
8 Ba 127	320 (4)	15.8	15.1	0.96	22	61	25	9
8 Ba 128	320 (4)	15.1	13.6	0.90	25	71	33	8
8 Ba 129	320 (4)	14.6	12.8	0.88	23	71	30	12
Mean of 6	320	14.52	12.93	0.890	25.5	75.0	36.2	9
Range of 5(a)	540	11.7-14.3	11.0-13.5	0.94-0.95	20-26	74-83	-	9-10
Mean of 5(a)	540	13.18	12.48	0.942	22.8	79.0	-	9
8 Ba 120	540 (4)	12.5	11.2	0.90	20	63	-	8
8 Ba 122	540 (4)	13.0	12.5	0.96	22	67	24	8
8 Ba 124	540 (4)	13.4	13.2	0.99	19	61	23	11
Mean of 8	540	13.10	12.41	0.945	21.9	73.2	23.5	9

(a) From screening program (ref. 1)
(1) Stabilized at 30°R and then at 140°R before stabilizing and testing at 30°R
(2) Stabilized at 30°R and then at 320°R before stabilizing and testing at 30°R
(3) Stabilized at 30°R and then at 540°R before stabilizing and testing at 30°R
(4) Stabilized at 30°R before stabilizing and testing at indicated temperature
(#) For comparison purposes only
* Ductility values from 8 Ba 143 (Tested under the same conditions but loads not recorded due to instrumentation malfunction)
- Not available

TABLE 8 TEST RESULTS, EFFECTS OF IRRADIATION, ALUMINUM 1099-H14 (TESTED AT 30°R)

Specimen	Irradiation (n/cm^2, E>0.5 Mev)	F_{tu} (Ksi)	F_{ty} 0.2% offset (Ksi)	F_{ty}/F_{tu}	Elongation in 0.5 in. (4D) (%)	Reduction of Area (%)	Fracture Stress (Ksi)	Modulus(#) (10^3 Ksi)
Mean of 14 (c)	None	37.25	12.00	0.319	57.9	65.4	92.6	10
8 Ba 147 (b)	5×10^{15}	44.9	19.8	0.44	56	63	94	12
8 Ba 165	5×10^{15}	47.8	20.8	0.44	53	67	116	7
8 Ba 188	5×10^{15}	45.6	20.2	0.44	55	68	108	16
Mean	5×10^{15}	46.10	20.27	0.440	54.7	66.0	106.0	12
8 Ba 153	7×10^{15}	38.3	17.4	0.45	55	67	81	10
8 Ba 131 (b)	4×10^{16}	50.0	28.9	0.58	42	50	85	19
8 Ba 155 (b)	5×10^{16}	46.9	31.3	0.67	45	56	80	15
8 Ba 113 (b)	5×10^{16}	50.9	34.7	0.68	40	47	81	17
8 Ba 161	5×10^{16}	51.2	36.2	0.71	41	55	84	12
Mean	5×10^{16}	49.67	34.07	0.687	42.0	52.7	81.7	15
8 Ba 87 (a)	1×10^{17}	49.2	43.3	0.88	46	54	87	-
8 Ba 97 (b)	1×10^{17}	56.3	35.2	0.62	30	60	98	12
8 Ba 117 (b)	1×10^{17}	52.7	43.1	0.82	31	51	86	14
8 Ba 132 (b)	1×10^{17}	50.8	38.5	0.76	35	53	77	12
Mean	1×10^{17}	52.25	40.02	0.770	35.5	54.5	87.0	13
8 Ba 96 (b)	3×10^{17}	55.8	48.2	0.86	19	27	67	12
8 Ba 146 (b)	3×10^{17}	62.4	55.1	0.88	26	40	81	17
8 Ba 157 (b)	3×10^{17}	51.3	45.3	0.88	27	48	69	9
Mean	3×10^{17}	56.50	49.53	0.873	24.0	38.3	72.3	13

(a) From screening program (ref. 1)

(b) Previously reported (ref. 7)

(c) From table 7

(#) For comparison purposes only

- Not determinable

TABLE 9 TEST RESULTS, EFFECTS OF IRRADIATION TEMPERATURE, ALUMINUM 1099 - H 14
(1×10^{17} n/cm^2, E > 0.5 MeV, TESTED AT IRRADIATION TEMPERATURE)

Specimen	Temp. (°R)	Ftu (Ksi)	F_{ty} 0.2% offset (Ksi)	F_{ty}/Ftu	Elongation in 0.5 in (4D) (%)	Reduction of Area (%)	Fracture Stress (Ksi)	Modulus (#) (10^3 Ksi)
Mean of 4 (c)	30	52.2	40.0	0.770	35.5	54.5	87.0	13
8 Ba 162	140	25.9	18.9	0.73	42	74	-	9
8 Ba 167	140	26.8	20.6	0.77	42	74	55	7
8 Ba 170	140	23.6	16.2	0.69	42	74	-	4
Mean	140	25.43	18.57	0.730	42.0	74.0	55	7
8 Ba 135 (b)	320	16.2	14.6	0.90	27	79	21	5
8 Ba 145 (b)	320	17.2	16.3	0.95	28	78	-	9
8 Ba 156 (b)	320	14.5	12.8	0.88	28	78	35	10
Mean	320	15.97	14.57	0.910	27.7	78.3	28.0	8
8 Ba 179	540	12.2	11.7	0.96	17	72	-	4
8 Ba 185	540	11.9	9.7	0.82	19	76	-	3
8 Ba 190	540	12.4	11.9	0.96	17	74	-	12
Mean	540	12.17	11.10	0.913	17.7	74.0	-	6

(c) From table 8

(b) Previously reported (ref. 7)

(#) For comparison purposes only

\- Not determinable

TABLE 10 TEST RESULTS, EFFECTS OF ANNEALING AND TEST TEMPERATURE, ALUMINUM 1099-H14
(1×10^{17} n/cm^2, E 0.5 MeV, AT 30°R, ANNEALED AND TESTED AT INDICATED TEMPERATURE)

Specimen	Annealing and Test Temp. (°R)	F_{tu} (Ksi)	F_{ty} 0.2% offset (Ksi)	F_{ty}/F_{tu}	Elongation in 0.5 in (4D) (%)	Reduction of Area (%)	Fracture Stress (Ksi)	Modulus (#) (10^3 Ksi)
Mean of 4 (c)	30 *	52.2	40.0	0.770	35.5	54.5	87.0	13
8 Ba 126 (b)	140	28.7	22.8	0.79	29	61	-	-
8 Ba 121 (b)	140	26.7	20.4	0.76	39	76	37	16
8 Ba 173	140	26.8	19.2	0.72	46	73	41	-
Mean	140	27.40	20.80	0.757	38.0	70.0	39.0	16
8 Ba 106 (b)	320	16.6	15.9	0.96	29	85	-	14
8 Ba 177	320	16.4	13.7	0.84	28	81	-	4
8 Ba 114	320	16.8	15.5	0.92	23	78	-	9
Mean	320	16.60	15.03	0.907	26.7	81.3	-	9
8 Ba 160	540	11.9	11.5	0.97	20	75	27	7
8 Ba 163	540	11.7	10.7	0.91	20	75	33	4
8 Ba 164	540	12.0	11.7	0.98	22	77	27	12
Mean	540	11.87	11.30	0.953	20.7	75.7	29.0	8

(b) Previously reported (ref. 7)
(c) From table 8

(#) For comparison purposes only
- Not determinable
* Not annealed after irradiation

TABLE 11 TEST RESULTS, EFFECTS OF ANNEALING, ALUMINUM 1099-H14
(1×10^{17} n/cm^2 E 0.5 MeV, AT 30°R, ANNEALED AT INDICATED TEMPERATURE, TESTED AT 30°R)

Specimen	Annealing Temp. (°R)	F_{tu} (Ksi)	F_{ty} 0.2% offset (Ksi)	F_{ty}/F_{tu}	Elongation in 0.5 in (4D) (%)	Reduction of Area (%)	Fracture Stress (Ksi)	Modulus (#) (10^3 Ksi)
Mean of 4 (c)	Not Annealed	52.2	40.0	0.770	35.5	54.5	87.0	13
8 Ba 140 (b)	140	45.2	28.9	0.64	39	53	64	14
8 Ba 178	140	54.5	34.4	0.63	43	58	93	15
8 Ba 181	140	46.1	28.5	0.62	46	58	84	16
Mean	140	48.60	30.60	0.630	42.7	56.3	80.3	15
8 Ba 186	320	44.2	23.9	0.54	47	62	85	18
8 Ba 189	320	44.4	24.1	0.54	43	59	76	3
8 Ba 200	320	37.4	16.5	0.44	58	62	78	12
Mean	320	42.00	21.50	0.507	49.3	61.0	79.7	11
8 Ba 187	540	45.5	16.2	0.36	63	61	96	3
8 Ba 193	540	43.4	15.9	0.37	58	58	75	13
8 Ba 198	540	40.4	10.4	0.26	58	59	79	3
Mean	540	43.10	14.17	0.330	59.7	59.3	83.3	6

(c) From table 8

(b) Previously reported (ref. 7)

(#) For comparison purposes only

\- Not determinable

TABLE 12 SCOPE OF TENSILE TEST PROGRAM FOR STUDYING THE EFFECTS OF IRRADIATION AT 30°R ON TITANIUM AND TITANIUM ALLOYS

MATERIAL	CONDITION	NUMBER SPECIMENS	EXPOSURE n/cm^2 (E 0.5 MeV)	REMARKS
Ti-55A	Annealed	3	6×10^{17}	(1) (2)
Ti-55A	Annealed	3	1×10^{18}	(1) (2)
Ti-5Al-2.5 Sn (ELI)	Annealed	3	1×10^{18}	(1) (2)
Ti-5Al-2.5 Sn (STD)	Annealed	3	1×10^{18}	(1)
Ti-6Al-4V	Annealed	3	1×10^{18}	(1) (2)
Ti-6Al-4V	Aged	3	1×10^{18}	(1)

(1) Data from tests at 30°R and 540°R without irradiation and at 30°R with 1×10^{17} n/cm^2 (E > 0.5 MeV) irradiation available from screening program (ref. 1).

(2) These tests completed at the end of this reporting period.

TABLE 13 TEST RESULTS, TITANIUM 55A-ANNEALED[b]

Specimen	Temp. (°R)	Irradiation (n/cm^2, E>0.5 MeV)	F_{tu} (Ksi)	F_{ty} 0.2% offset (Ksi)	F_{ty}/F_{tu}	Elongation in 0.5 in (4D) (%)	Reduction of Area (%)	Fracture Stress (Ksi)	Modulus[#] (10^3 Ksi)
Range of 5[a]	540	None	65.1-69.4	47.5-63.3	0.73-0.91	25-33	59-65	-	12-14
Mean of 5[a]	540	None	67.0	53.5	0.798	30.0	62.3	-	14
Range of 5[a]	30	None	167-172	118-124	0.71-0.73	33-34	51-54	-	16-20
Mean of 5[a]	30	None	169.4	122.0	0.722	33.3	53.0	-	18
Range of 3[a]	30	1×10^{17}	180-216	128-136	0.63-0.73	32-36	52-54	-	17-25
Mean of 3[a]	30	1×10^{17}	192.3	131.7	0.690	34.0	53.0	-	18
1 Aa 200	30	6×10^{17}	203	154	0.75	29	45	370	20
1 Aa 203	30	6×10^{17}	204	158	0.78	29	46	380	19
1 Aa 153	30	6×10^{17}	211	154	0.73	27	38	341	15
Mean	30	6×10^{17}	206.0	155.3	0.753	28.3	43.0	363.7	18
1 Aa 152	30	1×10^{18}	213	159	0.74	30	49	420	12
1 Aa 205	30	1×10^{18}	216	171	0.79	29	44	387	22
1 Aa 206	30	1×10^{18}	223	181	0.81	19	38	358	-
Mean	30	1×10^{18}	217.3	170.3	0.780	26.0	43.7	388.3	17

(a) From screening program (ref. 1)
(b) Previously reported (ref. 7)
(#) For comparison purposes only
- Not determinable

TABLE 14 TEST RESULTS, TITANIUM-5Al-2.5 Sn (ELI)-ANNEALED

Specimen	Temp. (°R)	Irradiation (n/cm^2 E>0.5 MeV)	F_{tu} (Ksi)	F_{ty} 0.2% offset (Ksi)	F_{ty}/F_{tu}	Elongation in 0.5 in (4D) (%)	Reduction of Area (%)	Fracture Stress (Ksi)	Modulus(#) (10^3 Ksi)
Range of 5(a)	540	None	118-133	104-119	0.88-0.91	12-19	39-46	169-171	15-20
Mean of 5(a)	540	None	126.4	113.4	0.896	16.0	42.2	170.0	15
Range of 5(a)	30	None	225-236	203-225	0.92-0.96	8-11	32-33	-	-
Mean of 5(a)	30	None	228.4	214.2	0.948	9.7	32.3	-	-
Range of 3(a)	30	1×10^{17}	222-225	211-215	0.95-0.96	11	31	-	17-18
Mean of 3(a)	30	1×10^{17}	223.3	213.0	0.953	11.0	31.0	-	18
8 Aa 49 (b)	30	1×10^{18}	268.0	262.1	0.98	6	22	-	22
8 Aa 55 (b)	30	1×10^{18}	270.9	263.1	0.97	6	25	359	23
8 Aa 60	30	1×10^{18}	252.6	250.0	0.99	6	27	347	22
Mean	30	1×10^{18}	263.8	258.4	0.980	6.0	24.7	353.0	22

(a) From screening program (ref. 1)

(#) For comparison purposes only

(b) Previously reported (ref. 7)

- Not determinable

TABLE 15 TEST RESULTS, TITANIUM 6 AL - 4V (ANNEALED)

Specimen	Temp. (°R)	Irradiation (n/cm^2, E>0.5 MeV)	F_{tu} (Ksi)	F_{ty} 0.2% offset (Ksi)	F_{ty}/F_{tu}	Elongation in 0.5 in (4D) (%)	Reduction of Area-(%)	Fracture Stress	Modulus(#) (10^3 Ksi)
Range of 5 (a)	540	None	142-145	134-141	0.94-0.97	13-14	42-48	-	14-15
Mean of 5 (a)	540	None	144.0	137.8	0.957	13.8	45.0	-	15
Range of 5 (a)	30	None	249-265	228-255	0.87-0.97	7-10	27-36	-	17-17
Mean of 5 (a)	30	None	260.4	243.2	0.934	7.6	30.4	-	17
Range of 3 (a)	30	1×10^{17}	265-290	254	0.95	5-6	37-38	-	-
Mean of 3 (a)	30	1×10^{17}	273.7	254	0.95	5.7	37.3	-	-
2 Ac 54	30	1×10^{18}	302.7	289.4	0.96	4	34	456	20
2 Ac 55	30	1×10^{18}	332.9	314.5	0.95	4	34	506	25
2 Ac 56	30	1×10^{18}	325.0	294.7	0.91	6	34	494	32
Mean	30	1×10^{18}	320.2	299.5	0.940	4.7	34.0	485.3	26

(a) From screening program (ref. 1)

(#) For comparison purposes only

- Not determinable

TABLE 16 FATIGUE TEST PROGRAM (SCOPE)

Material	No. Specimens (Max)	Test Type	Exposure °R	Exposure Cpm (min)	Exposure Location
Ti-55A	9	Fatigue During Exposure	540	6	Out-of-pile
Ti-55A	9	Fatigue During Exposure	30	6	Out-of-pile
Ti-55A	9	Fatigue During Exposure	30	6	In-pile
Ti-5Al-2.5 Sn (Eli)	9	Fatigue During Exposure	540	6	Out-of-pile
Ti-5Al-2.5 Sn (Eli)	9	Fatigue During Exposure	30	6	Out-of-pile
Ti-5Al-2.5 Sn (Eli)	9	Fatigue During Exposure	30	6	In-pile
Ti-5Al-2.5 Sn (Std)	9	Fatigue During Exposure	540	6	Out-of-pile
Ti-5Al-2.5 Sn (Std)	9	Fatigue During Exposure	30	6	Out-of-pile
Ti-5Al-2.5 Sn (Std)	9	Fatigue During Exposure	30	6	In-pile
Ti-6Al-4V (Ann)	9	Fatigue During Exposure	540	6	Out-of-pile
Ti-6Al-4V (Ann)	9	Fatigue During Exposure	30	6	Out-of-pile
Ti-6Al-4V (Ann)	9	Fatigue During Exposure	30	6	In-pile
Ti-6Al-4V (Aged)	9	Fatigue During Exposure	540	6	Out-of-pile
Ti-6Al-4V (Aged)	9	Fatigue During Exposure	30	6	Out-of-pile
Ti-6Al-4V (Aged)	9	Fatigue During Exposure	30	6	In-pile

Material	No. Specimens (Max)	Test Type	Exposure n/cm^2 (E>0.5 MeV)	Exposure °R	Post-Exposure °R	Post-Exposure Cpm (min)
Ti-55A	9	Post-Exposure Fatigue	0	30	30	6
Ti-55A	9	Post-Exposure Fatigue	1×10^{17}	30	30	6
Ti-5Al-2.5 Sn (Eli)	9	Post-Exposure Fatigue	0	30	30	6
Ti-5Al-2.5 Sn (Eli)	9	Post-Exposure Fatigue	1×10^{17}	30	30	6
Ti-5Al-2.5 Sn (Std)	9	Post-Exposure Fatigue	0	30	30	6
Ti-5Al-2.5 Sn (Std)	9	Post-Exposure Fatigue	1×10^{17}	30	30	6
Ti-6Al-4V (Ann)	9	Post-Exposure Fatigue	0	30	30	6
Ti-6Al-4V (Ann)	9	Post-Exposure Fatigue	1×10^{17}	30	30	6
Ti-6Al-4V (Aged)	9	Post-Exposure Fatigue	0	30	30	6
Ti-6Al-4V (Aged)	9	Post-Exposure Fatigue	1×10^{17}	30	30	6

9 FIGURES

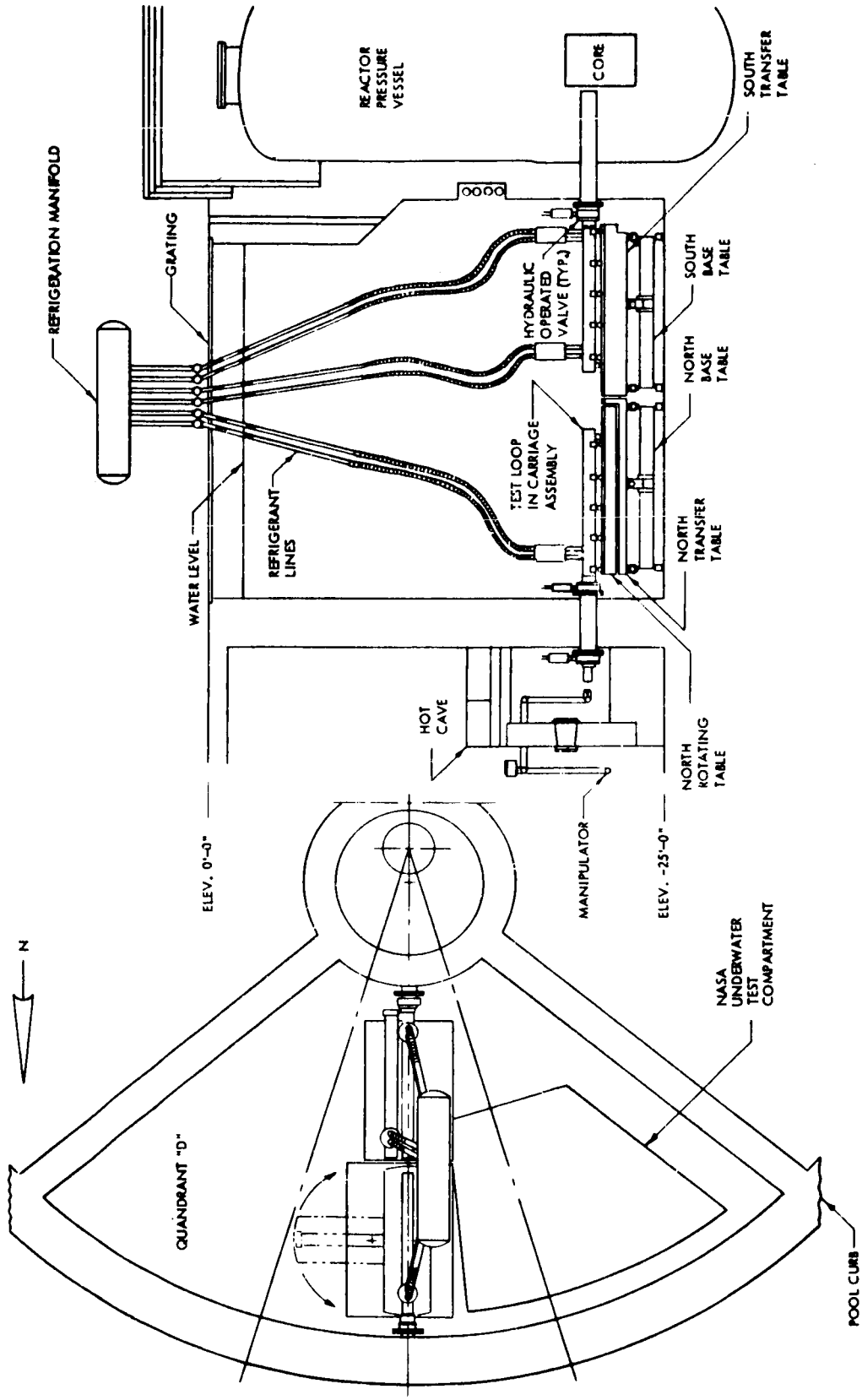

FIGURE 1 SYSTEM LAYOUT

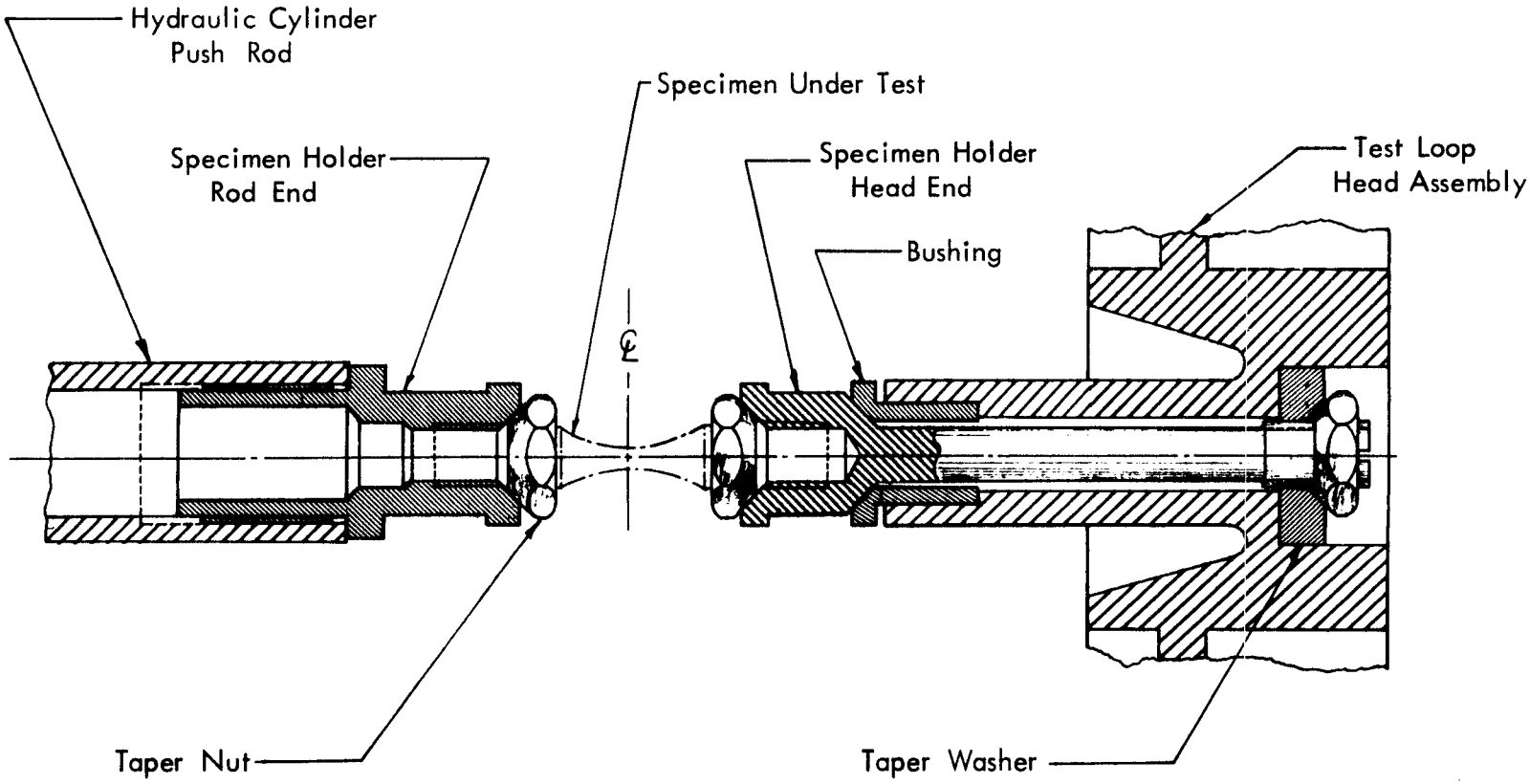

FIGURE 2 SPECIMEN HOLDER DESIGN

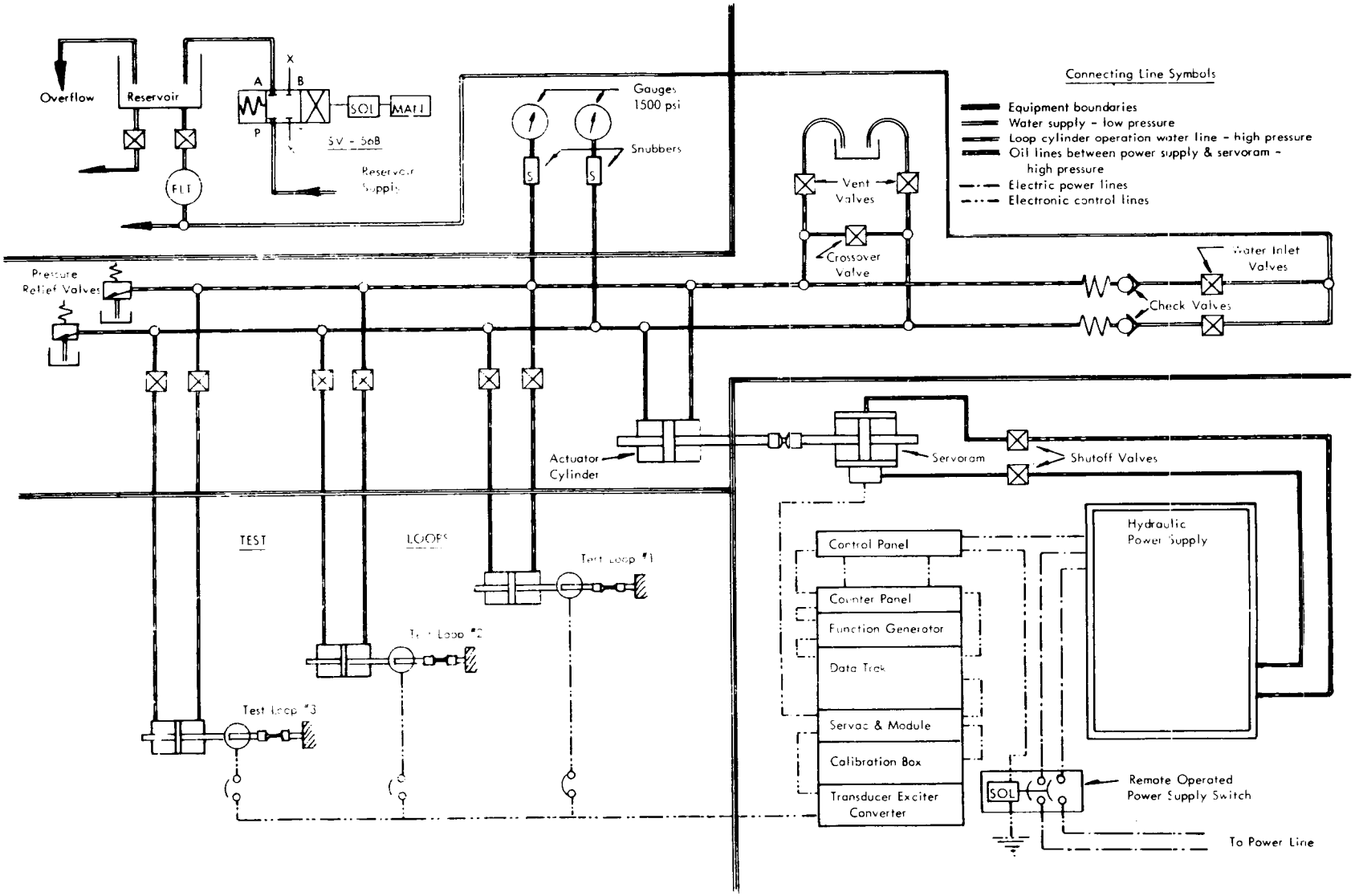

FIGURE 3 LOAD CONTROL SYSTEM (SCHEMATIC)

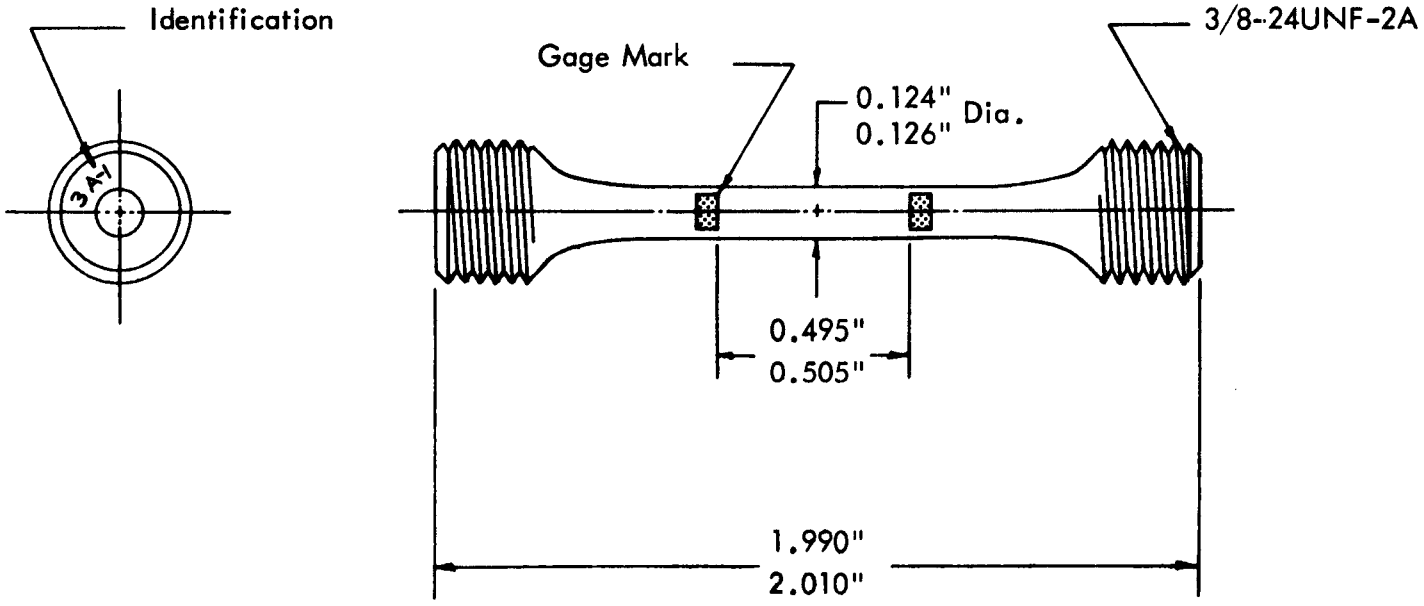

Note: Diameter at gage marks shall be center diameter + $\begin{matrix}0.002"\\0.004"\end{matrix}$.

FIGURE 4 TENSILE SPECIMEN

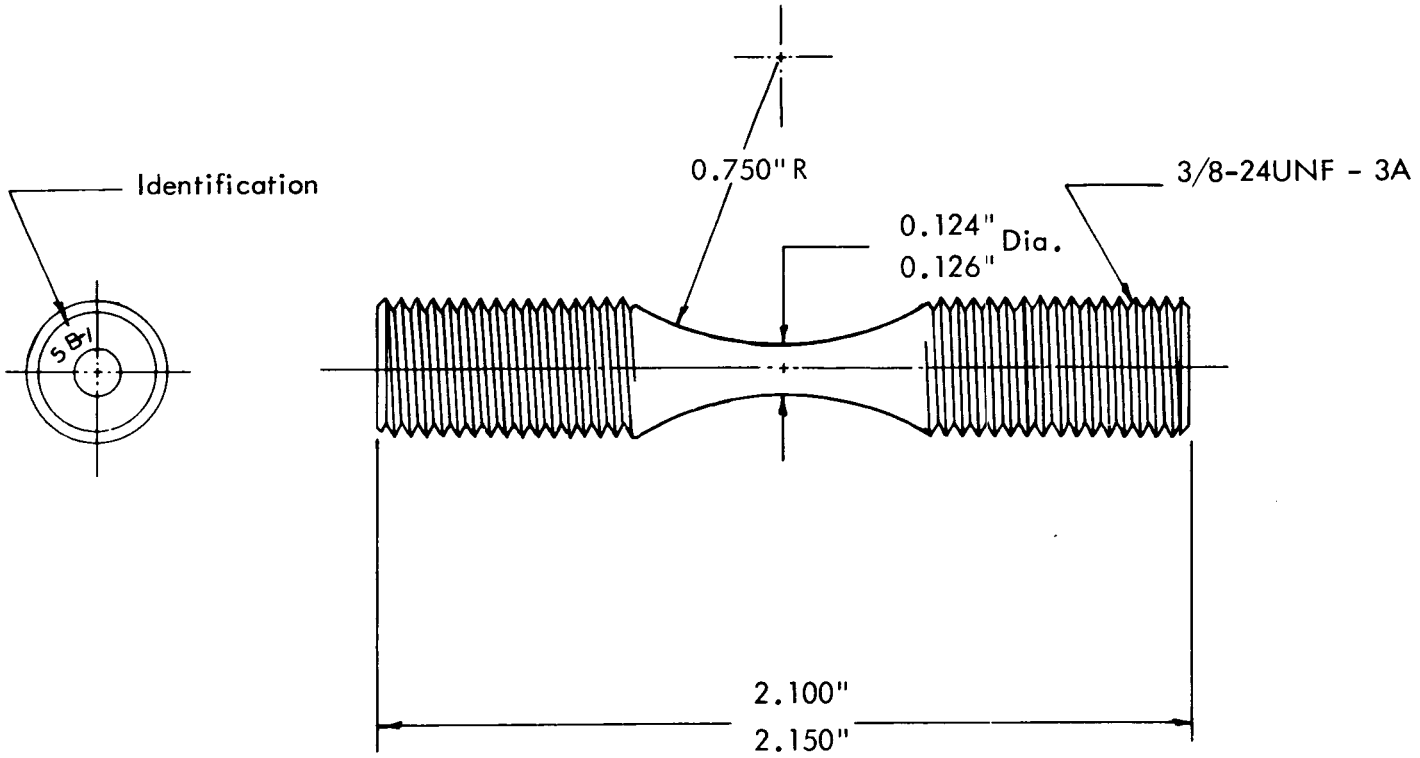

FIGURE 5 FATIGUE SPECIMEN

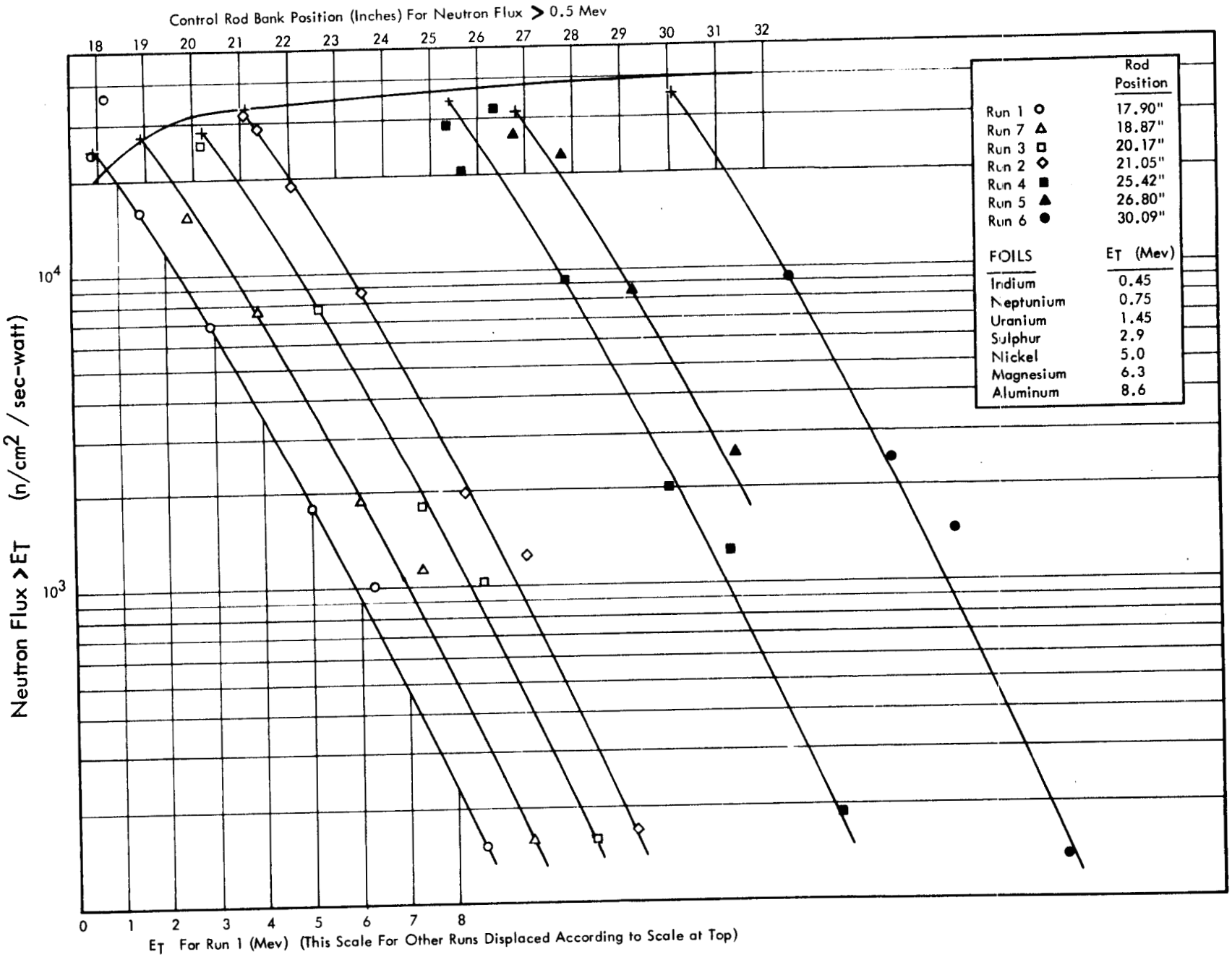

FIGURE 6 NEUTRON FLUX>E_T VS. E_T AND NEUTRON FLUX >0.5 MEV VS. CONTROL ROD BANK POSITION

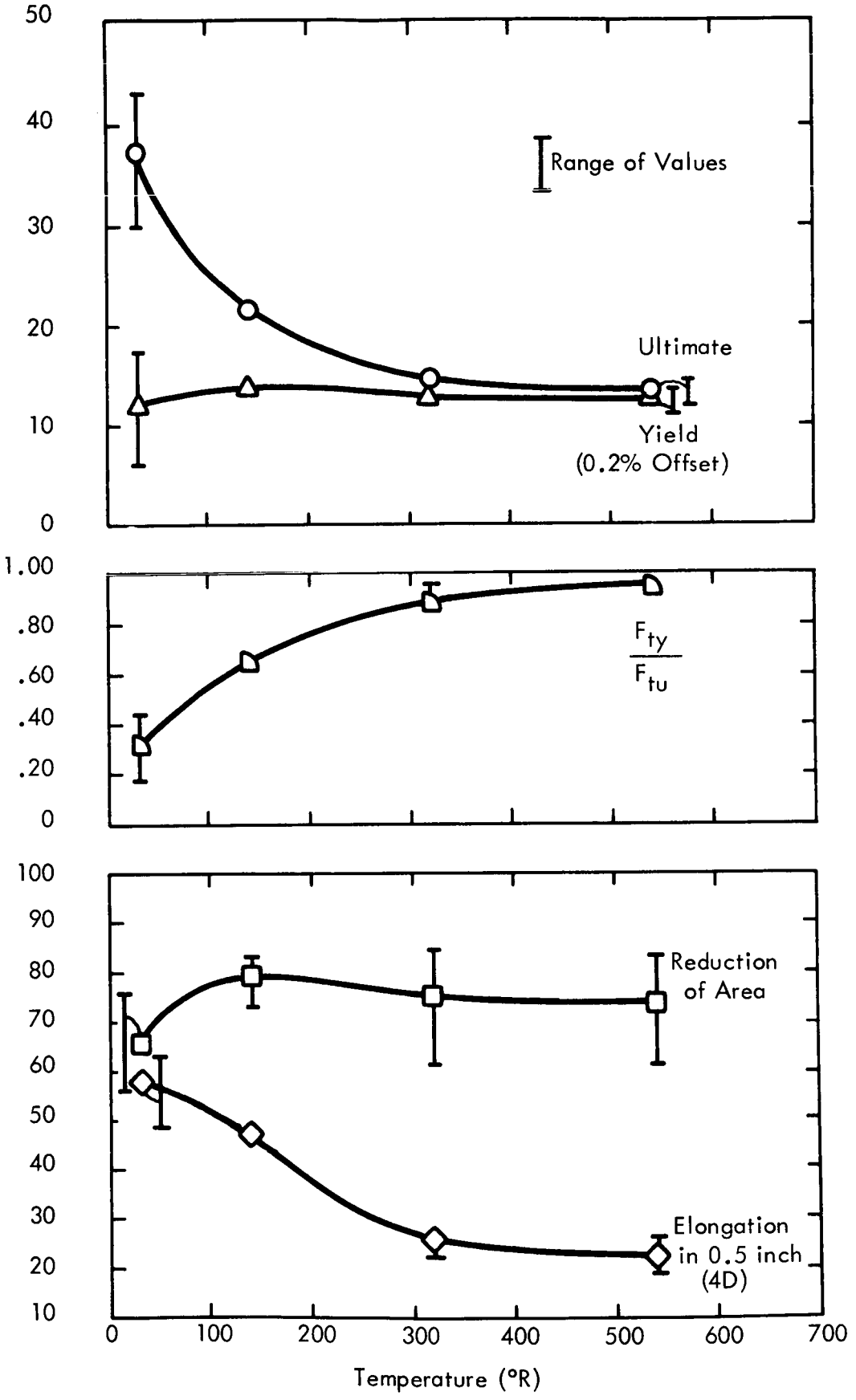

FIGURE 7 TEMPERATURE DEPENDENCE OF TENSILE PROPERTIES ALUMINUM 1099-H14, UNIRRADIATED

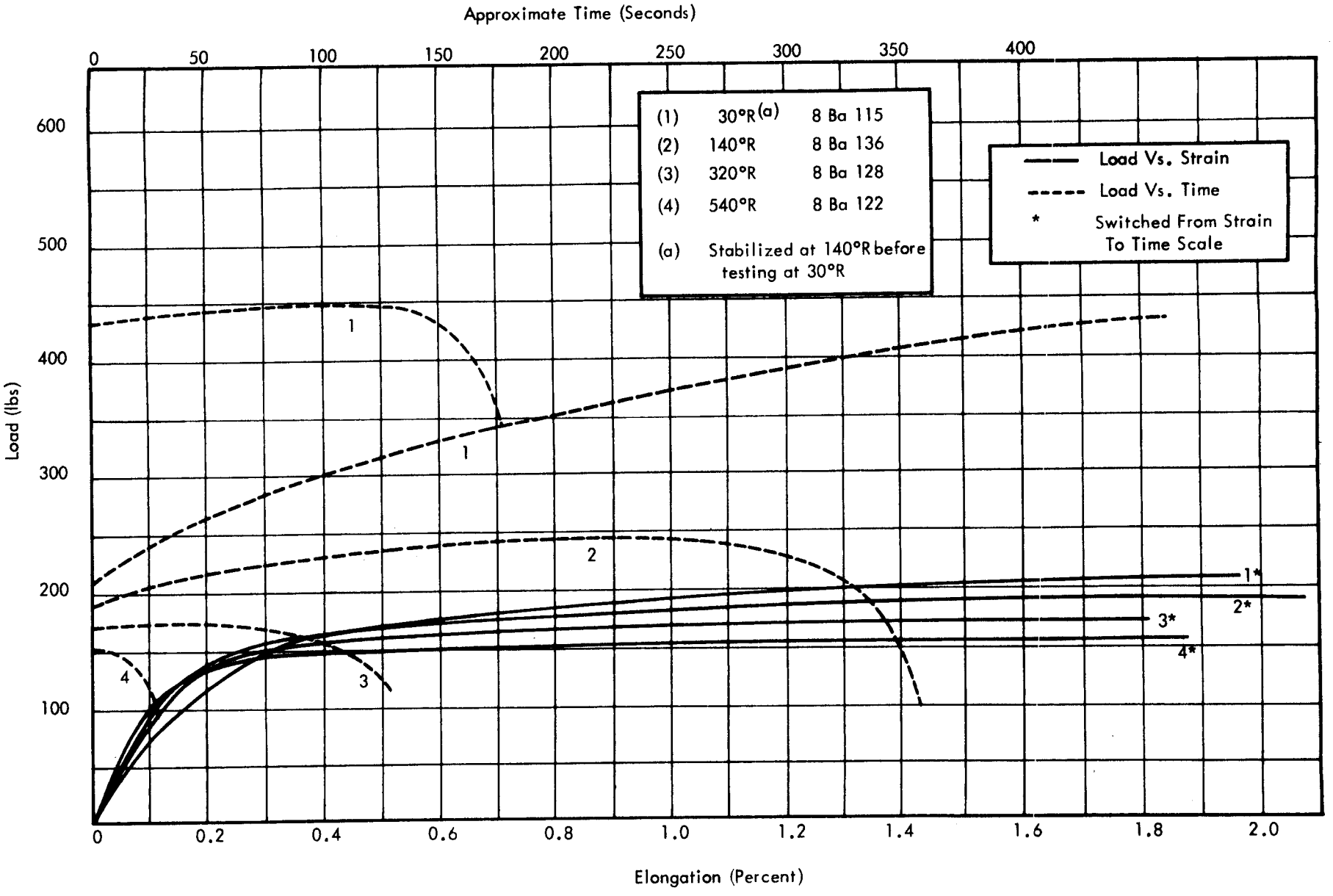

FIGURE 8 TYPICAL LOAD-ELONGATION CURVES, AT VARIOUS TEMPERATURES, FOR ALUMINUM 1099-H14, UNIRRADIATED

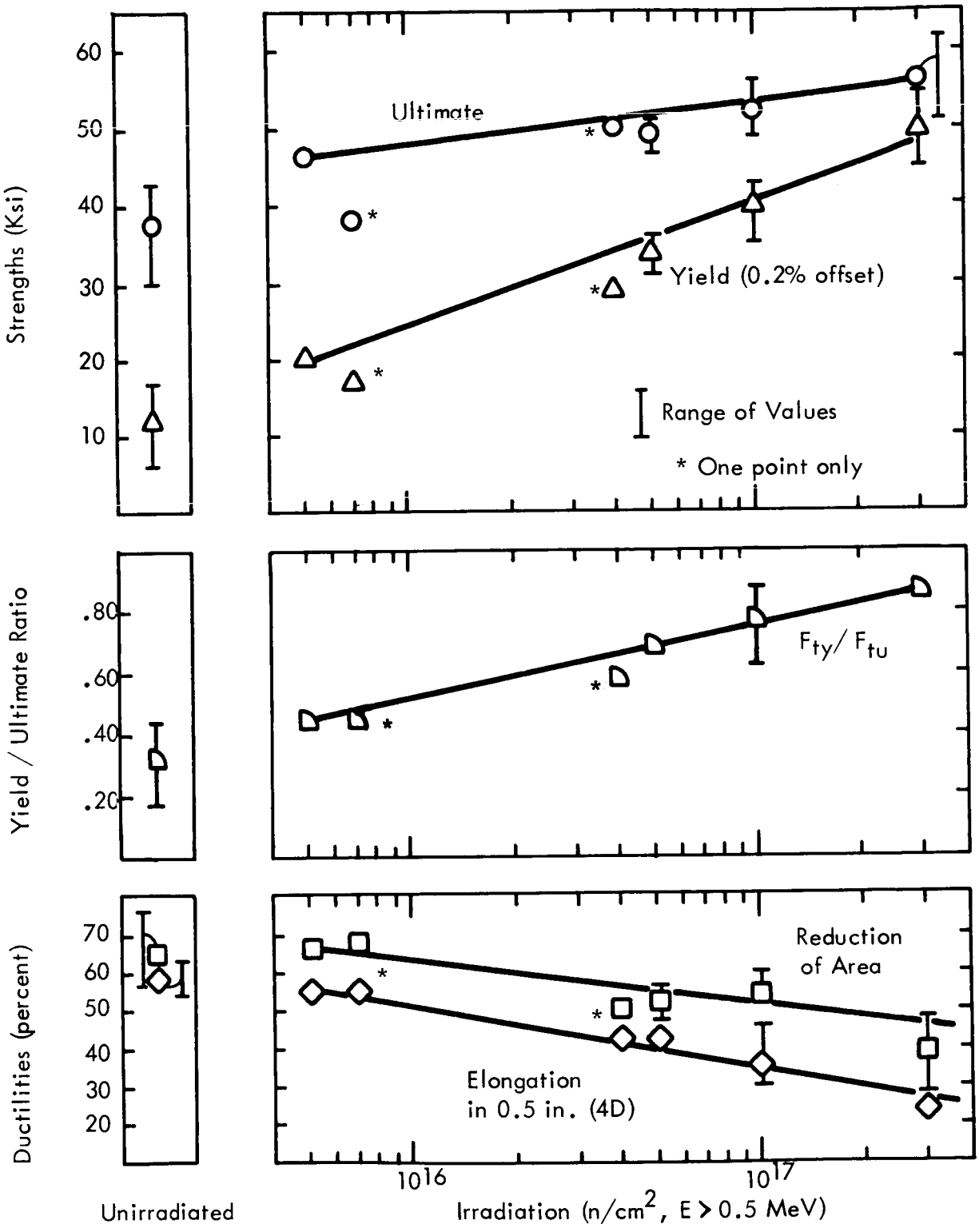

FIGURE 9 EFFECTS OF IRRADIATION AT 30°R ON ALUMINUM 1099-H14

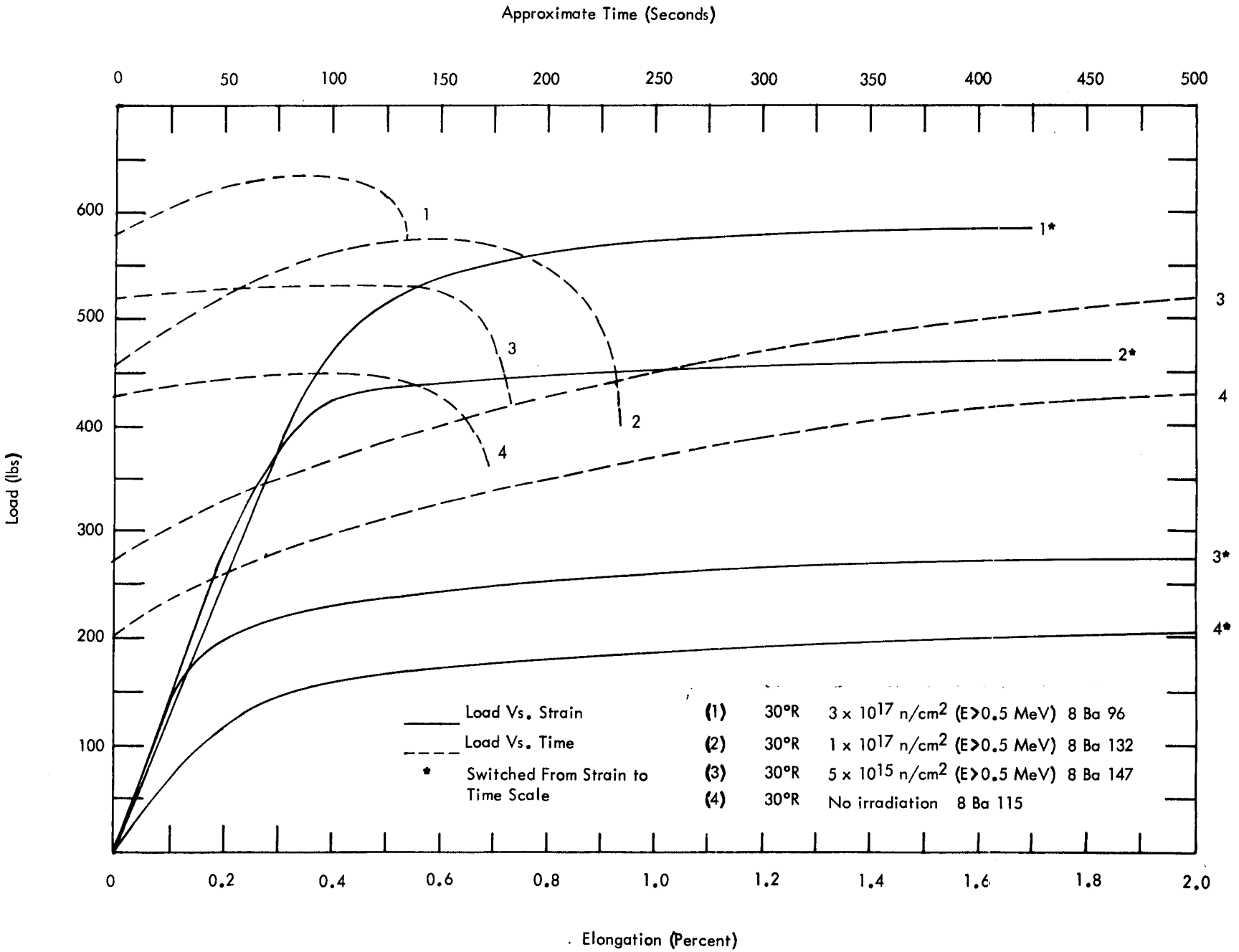

FIGURE 10 TYPICAL LOAD ELONGATION CURVES, AT VARIOUS IRRADIATION LEVELS, FOR ALUMINUM 1099 - H 14

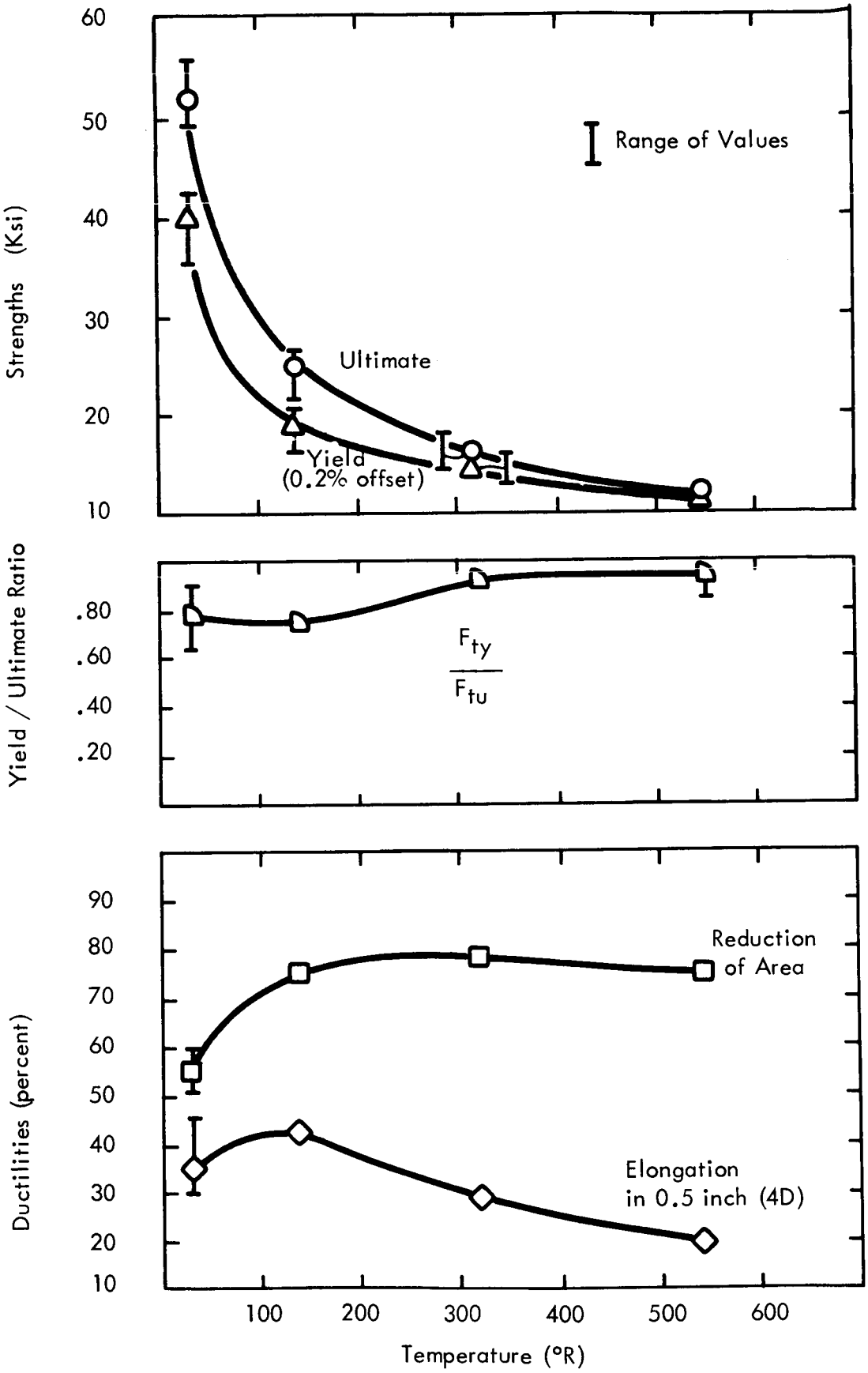

FIGURE 11 EFFECTS OF IRRADIATION TEMPERATURE, IRRADIATED TO 10^{17} n/cm^2 AT INDICATED TEMPERATURE, TESTED AT IRRADIATION TEMPERATURE, ALUMINUM 1099-H14

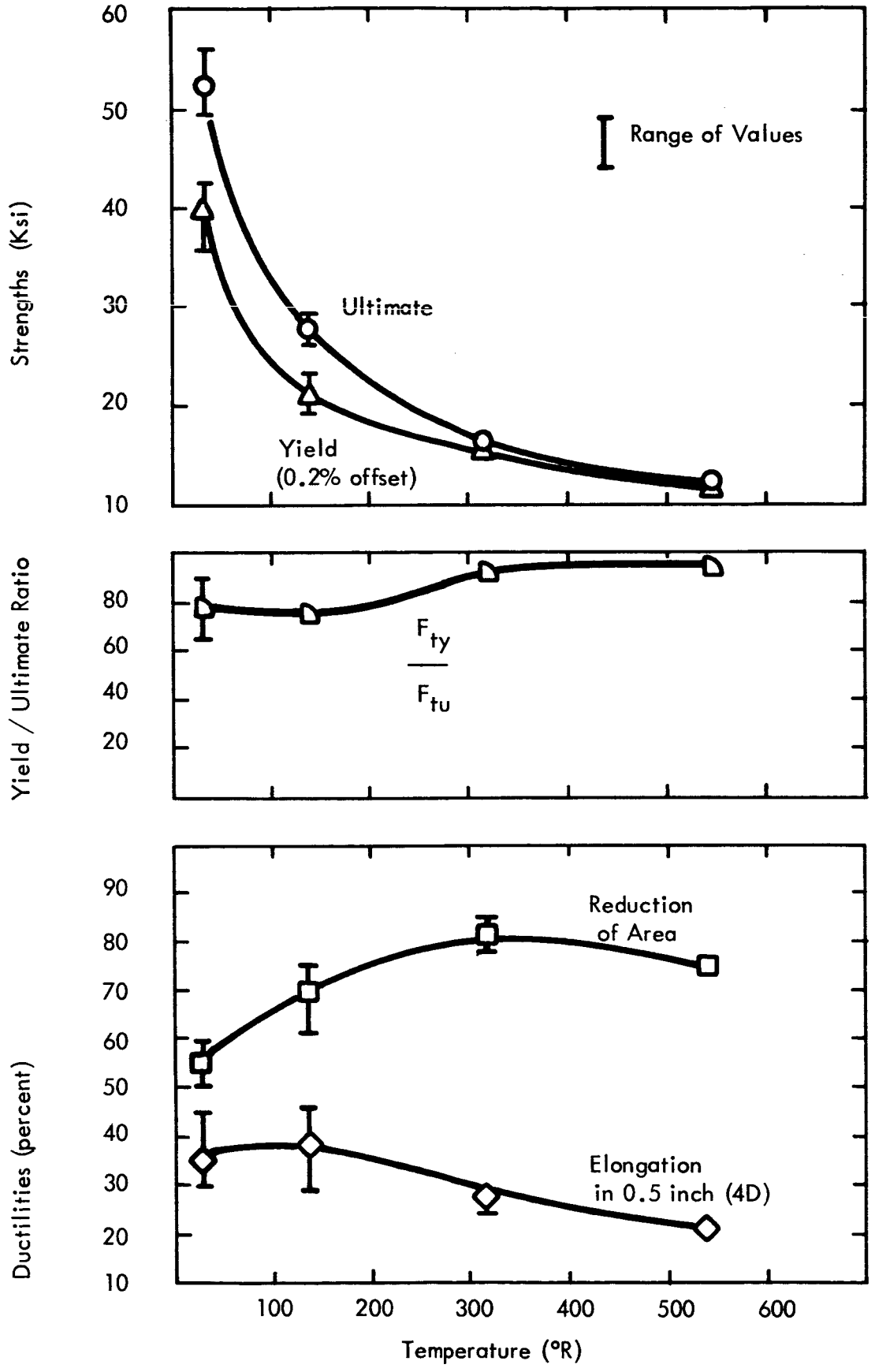

FIGURE 12 EFFECTS OF ANNEALING AND TEST TEMPERATURE, IRRADIATED TO 10^{17} n/cm^2 AT 30°R, ANNEALED AND TESTED AT INDICATED TEMPERATURE, ALUMINUM 1099-H14

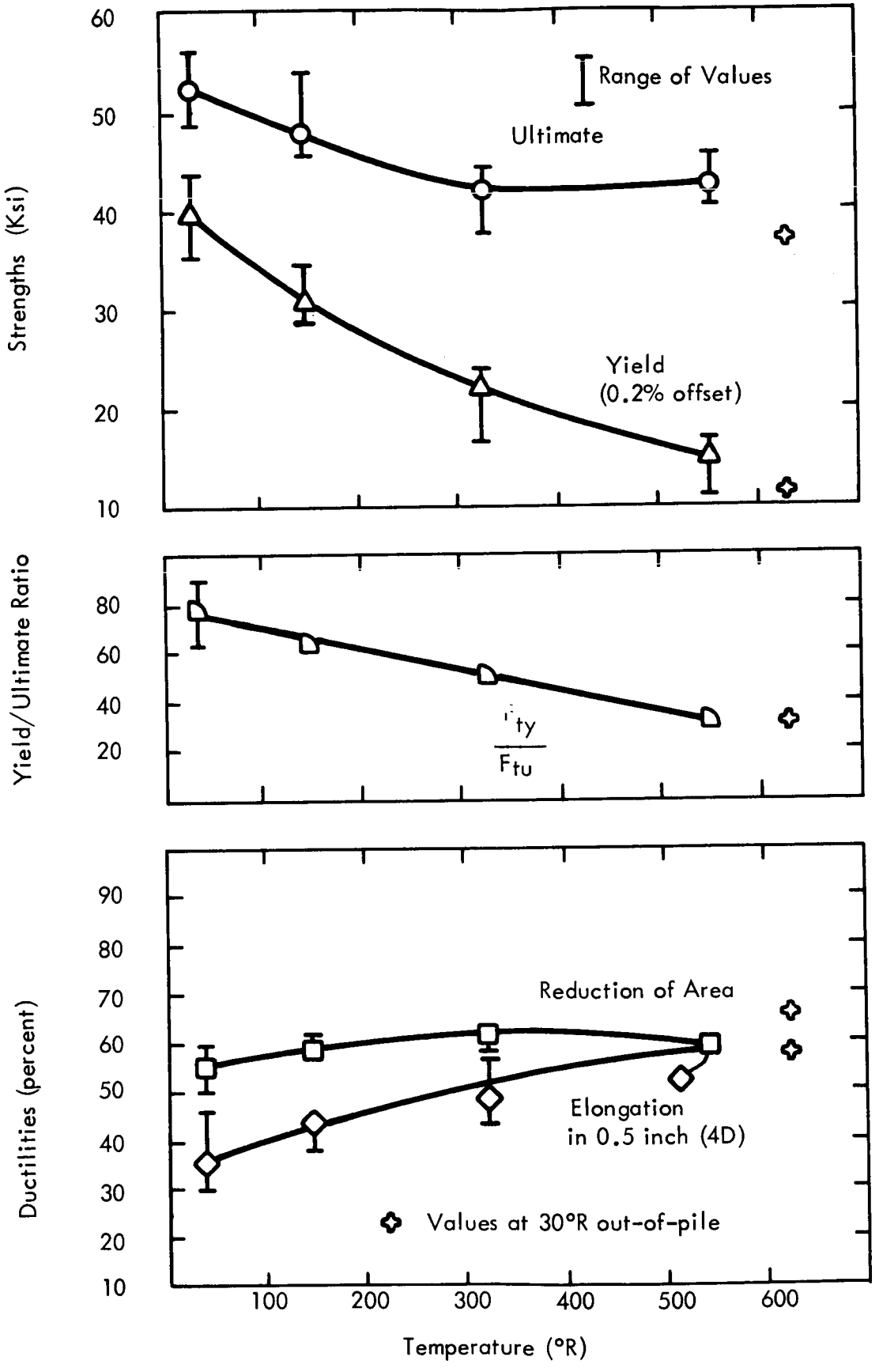

FIGURE 13 EFFECTS OF ANNEALING TEMPERATURE, IRRADIATED TO 10^{17} n/cm^2 AT 30°R, ANNEALED AT INDICATED TEMPERATURE, TESTED AT 30°R, ALUMINUM 1099-H14

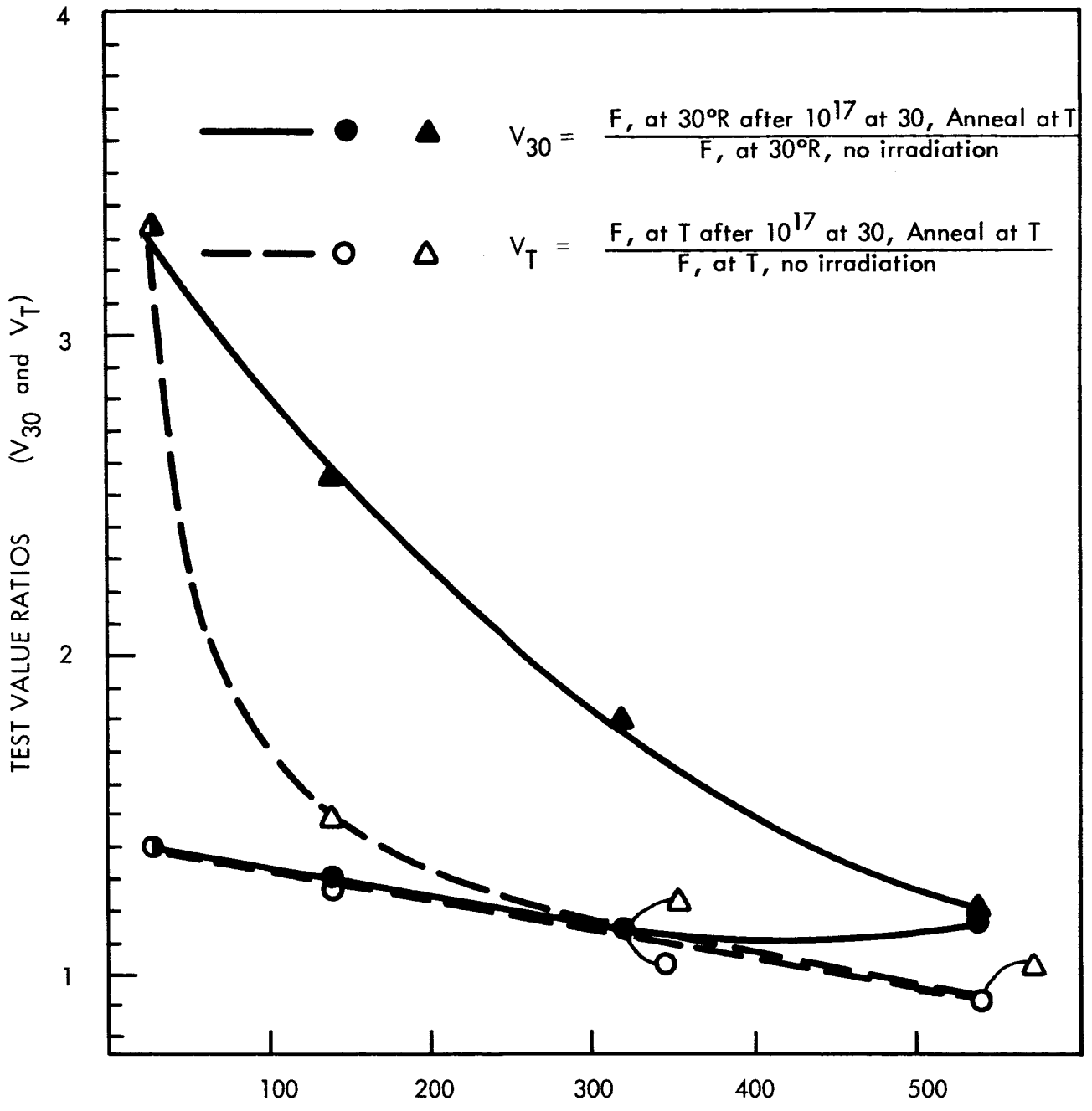

FIGURE 14 COMPARISON OF TEST RESULTS, ALUMINUM 1099-H14, ANNEALED AND TESTED AT INDICATED TEMPERATURE VS. ANNEALED AT INDICATED TEMPERATURE, TESTED AT 30°R

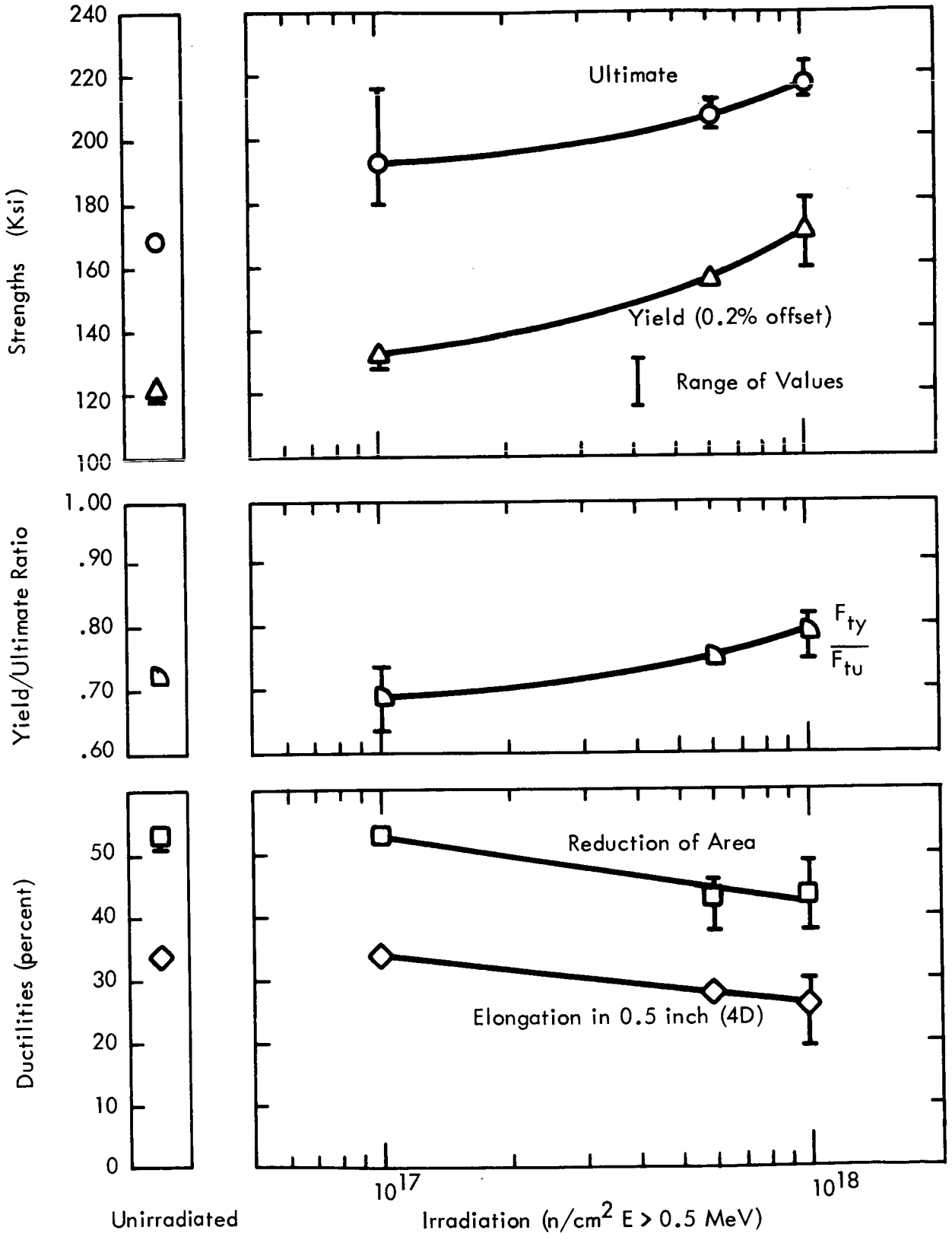

FIGURE 15 EFFECTS OF IRRADIATION AT 30°R ON TITANIUM 55A

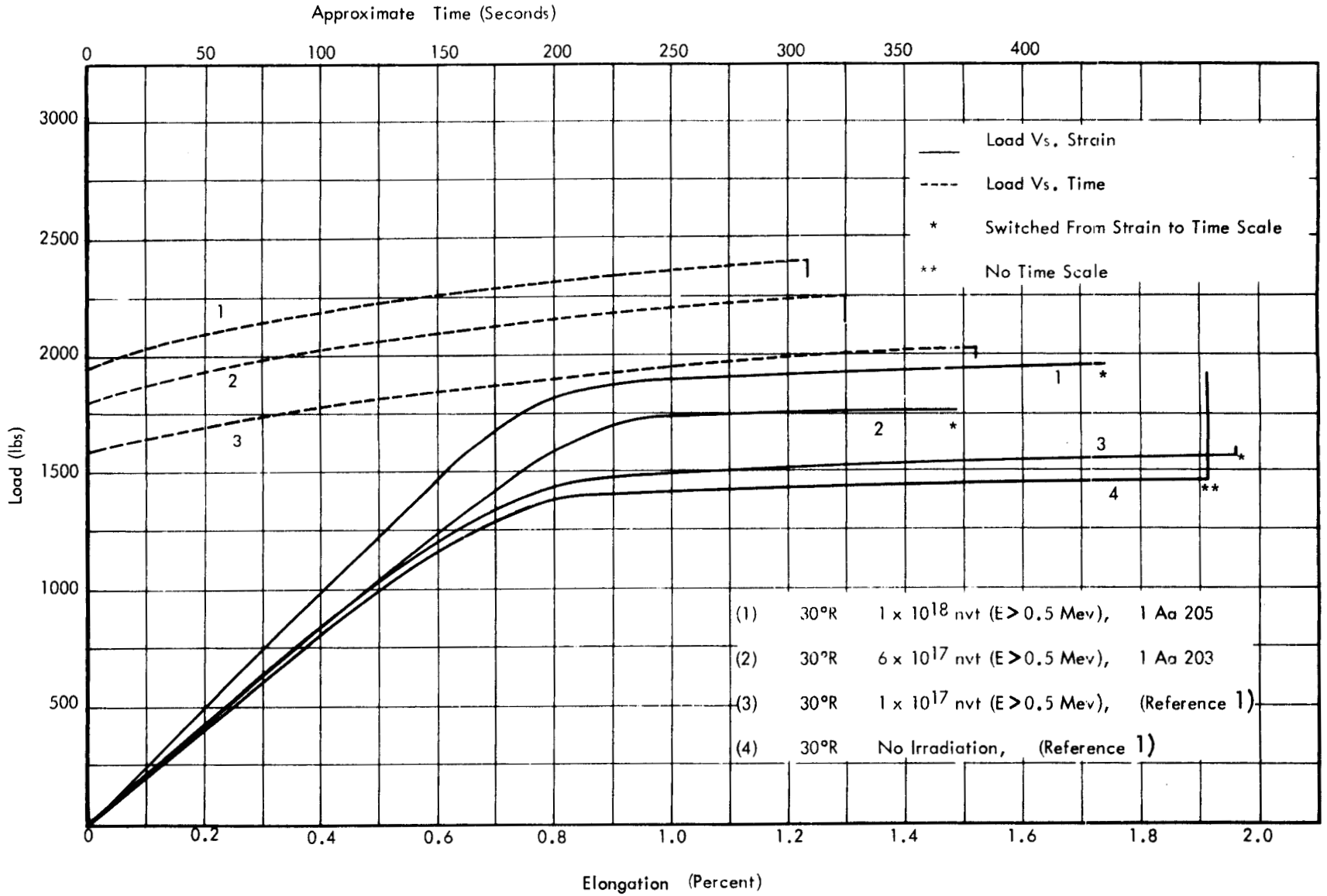

FIGURE 16 TYPICAL LOAD-ELONGATION CURVES FOR TITANIUM 55A

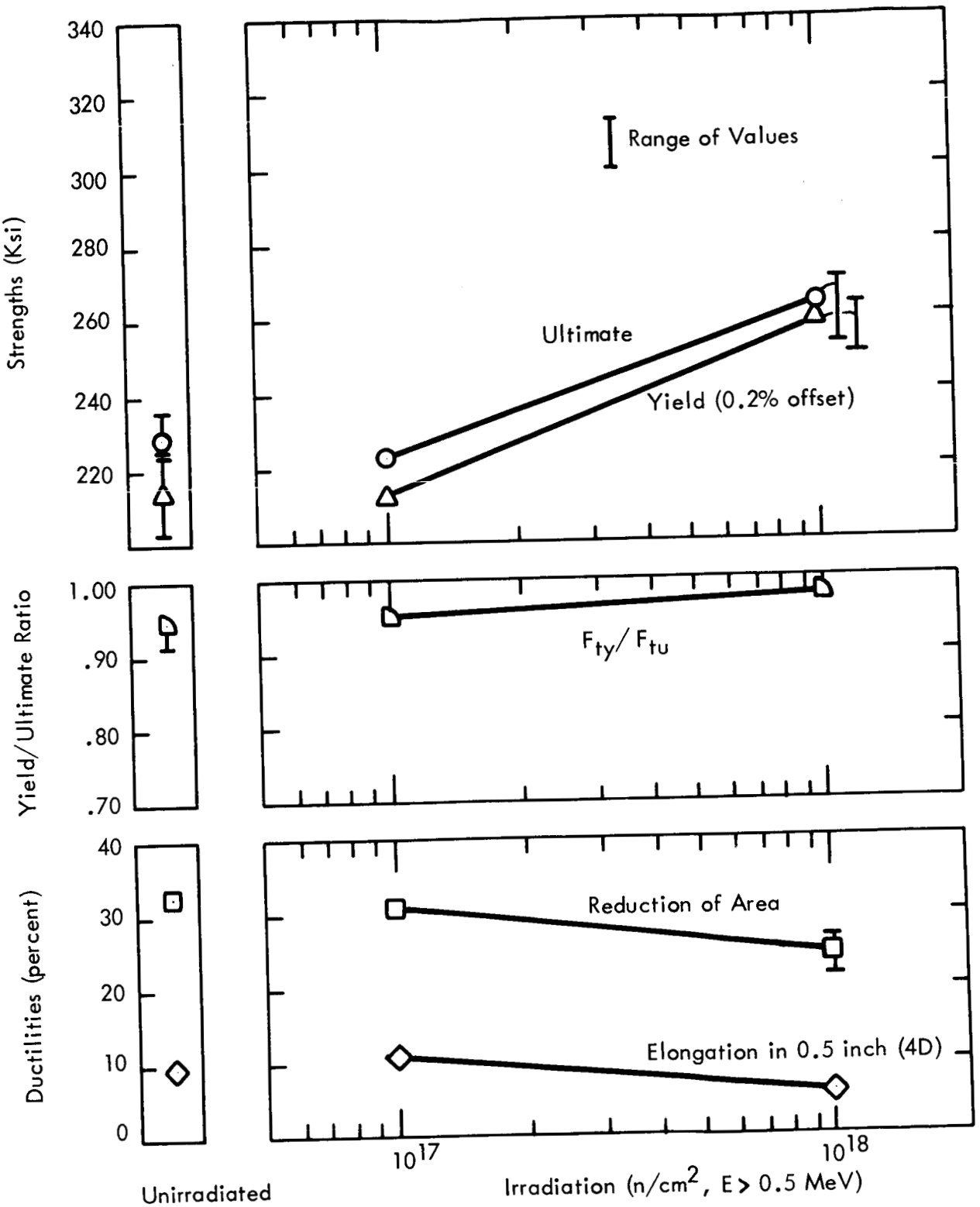

FIGURE 17 EFFECTS OF IRRADIATION AT 30°R ON TITANIUM 5 Al-2.5 Sn (ELI)

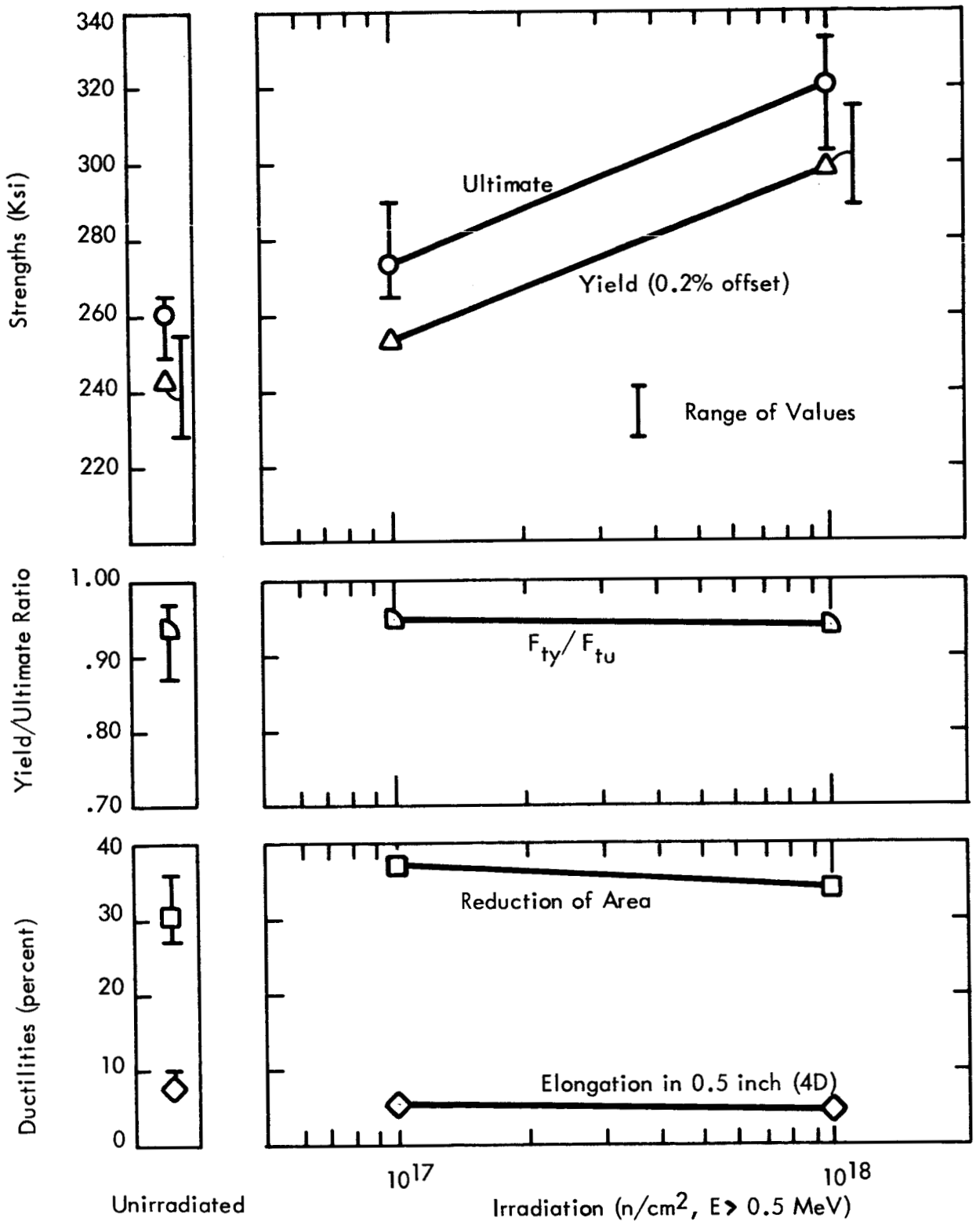

FIGURE 18 EFFECTS OF IRRADIATION AT 30°R ON TITANIUM 6 Al-4V (ANNEALED)

ABSTRACT

This is the fourth quarterly report summarizing, to date, studies (under Contract NAS 3-7985) of the effects of nuclear radiation on materials at cryogenic temperatures. These studies include the effects of (1) 10^{18} n/cm^2 (E > 0.5 MeV) at 30°R on tensile properties of titanium base alloys; (2) irradiation temperature (30°R to 540°R) on tensile properties of Aluminum 1099-H14 following irradiations up to 3×10^{17} n/cm^2 (E > 0.5 MeV); (3) annealing following irradiation at 30°R on axial, low-cycle fatigue properties of titanium base alloys; and (5) temperature (140°R and 540°R) on tensile properties of Titanium 55A and Aluminum 7178. This report presents the complete test results from the tensile testing of Aluminum 1099-H14 and Titanium Alloys 55A, 5-2 1/2 (ELI) and 6-4 (ANNEALED). Equipment maintenance, modification to existing test equipment and preparations for in-pile fatigue testing are described.